Hindawi Publishing Corporation
Journal of Biomedicine and Biotechnology
Volume 2010, Article ID 491217, 30 pages
doi:10.1155/2010/491217

Research Article

Microarray Detection Call Methodology as a Means to Identify and Compare Transcripts Expressed within Syncytial Cells from Soybean (*Glycine max*) Roots Undergoing Resistant and Susceptible Reactions to the Soybean Cyst Nematode (*Heterodera glycines*)

Vincent P. Klink,[1] Christopher C. Overall,[2,3,4] Nadim W. Alkharouf,[5] Margaret H. MacDonald,[2] and Benjamin F. Matthews[2]

[1] *Department of Biological Sciences, Harned Hall, Mississippi State University, Mississippi State, MS 39762, USA*
[2] *United States Department of Agriculture, Soybean Genomics and Improvement Laboratory, Building 006, Beltsville, MD 20705, USA*
[3] *Department of Bioinformatics and Computational Biology, George Mason University, Manassas, VA 20110, USA*
[4] *Department of Information Technology, College of Computing and Informatics, University of North Carolina-Charlotte, Charlotte, NC 28223, USA*
[5] *Department of Computer and Information Sciences, Jess and Mildred Fisher College of Science and Mathematics, Towson University, 7800 York Road, Towson, MD 21252, USA*

Correspondence should be addressed to Vincent P. Klink, vklink@biology.msstate.edu

Received 23 April 2009; Revised 23 September 2009; Accepted 14 February 2010

Academic Editor: Tanya Parish

Background. A comparative microarray investigation was done using detection call methodology (DCM) and differential expression analyses. The goal was to identify genes found in specific cell populations that were eliminated by differential expression analysis due to the nature of differential expression methods. Laser capture microdissection (LCM) was used to isolate nearly homogeneous populations of plant root cells. *Results*. The analyses identified the presence of 13,291 transcripts between the 4 different sample types. The transcripts filtered down into a total of 6,267 that were detected as being present in one or more sample types. A comparative analysis of DCM and differential expression methods showed a group of genes that were not differentially expressed, but were expressed at detectable amounts within specific cell types. *Conclusion*. The DCM has identified patterns of gene expression not shown by differential expression analyses. DCM has identified genes that are possibly cell-type specific and/or involved in important aspects of plant nematode interactions during the resistance response, revealing the uniqueness of a particular cell population at a particular point during its differentiation process.

1. Introduction

Microarray analyses are a way to study the expression of thousands of genes simultaneously. Microarray analyses are important because they can provide information on genes that are expressed differentially between a control and an experimental sample [1]. However, part of the problem of differential expression methodology is that genes must be expressed in both sample types, the experimental and control samples, for statistical analyses to be possible. Without gene expression data available for a probe set in each sample, the probe set will be discarded by the analysis procedure. The drawback of the differential expression methodology, therefore, is obvious when specific cell types with vastly different identities are being compared [2].

Microarray analyses, however, do provide useful information on the transcripts that are present or absent within samples [3]. Detection call methodology (DCM) reveals the types of transcripts that are present or absent within samples. The DCM is typically used on a single array to

answer whether a transcript of a particular gene is present or absent in a sample. Several recent papers have used DCM successfully to understand transcription in various experimental systems [4–6]. The DCM is useful when cost is an issue because the method can be performed on a single array. More importantly, DCM can be used to compare transcripts between different cell types or of the same cell type at different points during a time course [2, 3, 7]. None of these examples compared detection calls during a pathological infection. Nonetheless, DCM can provide extremely useful information about the samples under investigation, especially in the analysis of plant pathological systems where a pathogen interacts intimately with a specific cell population within a complex tissue or organ (e.g., root).

The infection of plants by parasitic nematodes is a major agricultural problem that is currently poorly understood (reviewed in [8–12]). Infection results in damage totaling 157 billion U.S. dollars, annually [13]. Among the most costly is *Heterodera glycines* infection of *Glycine max*, accounting for an estimated $460 to $818 million in production losses annually in the U.S. [14]. The *G. max-H. glycines* system is a powerful research tool because both resistant and susceptible reactions can be studied in the same genotype (e.g., *G. max*$_{[PI\ 548402/Peking]}$). Information learned through its genetic and genomic studies can be translated directly to improve resistance in one of the most important global agriculturally relevant plants.

The genetic basis of *G. max* to overcome *H. glycines* infection (an incompatible reaction resulting in resistance) is complex (reviewed in [15]). Several recessive resistance loci (*rhg1*, *rhg2,* and *rhg3*) [16] and dominant resistance loci (*Rhg4*) [17] and (*Rhg5*) [18] have been identified (reviewed in [15]). The understanding of resistance to *H. glycines* has also been aided by other genetic marker technology (e.g., quantitative trait loci (QTL) mapping). Those studies have identified QTLs that map to 17 linkage groups. *G. max*$_{[PI\ 548402/Peking]}$ has nine QTLs that map to different linkage groups (reviewed in [15]). One of those QTLs present in *G. max*$_{[PI\ 548402/Peking]}$ that maps to linkage group G explains more than 50% of resistance to *H. glycines* [19]. It also is responsible for resistance to several different populations of *H. glycines*. The major QTL that is located on linkage group G was identified using the RFLP marker C006V and is designated as *rhg1* [20]. Further studies have shown that molecular marker Satt309 is only 0.4 centiMorgans from *rhg1* [21]. Importantly, much of the resistance that has been bred into elite *G. max* varieties originates from the *G. max*$_{[PI\ 548402/Peking]}$ genotype.

Genomic approaches have also identified transcriptional changes in whole roots during infection [22–26]. Importantly, a time course microarray analysis was used to investigate the *G. max-H. glycines* interaction [23]. The analysis demonstrated that differential expression of genes was occurring in *G. max* roots undergoing a compatible reaction, a reaction that results in susceptibility. The analysis used time points both prior to and after feeding site selection [23]. Importantly, the differential expression of genes was occurring in *G. max* roots even before the nematodes had selected their feeding sites [23]. Thus, the plant is reacting in important ways to the presence of the nematode before the nematodes have begun to initiate the formation of their feeding sites during a compatible reaction.

The *G. max-H. glycines* interaction is an exceptional model because it is possible to compare gene expression occurring during incompatible (resistant) and compatible reactions. The experiments are possible because even resistant genotypes like *G. max*$_{[PI\ 548402/Peking]}$ undergo infection [12, 25–33]. The comparisons can be made because well-defined incompatible and compatible *H. glycines* races (populations) are available [12, 25, 26, 31–35]. A time course microarray analysis has examined *H. glycines* infection during both an incompatible and a compatible reaction in whole roots at time points both prior to and after nematodes have established feeding sites [25]. Importantly, those microarray analyses were performed in the same *G. max* genotype (e.g. *G. max*$_{[PI\ 548402/Peking]}$) by using incompatible and compatible populations of *H. glycines* [25, 26]. Thus, no possibility existed for *G. max* genotype differences complicating the identification of important gene expression events during those reactions. The analyses have shown that *G. max* behaves differently as it undergoes the incompatible or compatible reaction and these differences in gene expression are detectable as early as 12 hours post infection (hpi) [25]. The 12 hpi time point is a point before the nematode has selected its feeding site. The analyses also showed how expression of *G. max*$_{[PI\ 548402/Peking]}$ genes differs over time between roots undergoing an incompatible or compatible reactions.

The aforementioned investigations were not designed to study gene expression of the syncytium. However, several labs have made histological studies of the infection process. The studies showed that *H. glycines* infest the roots and migrate through the cortex during the early stages of the infestation process. After 24 hpi the nematodes reach the stele where they select and establish their feeding sites [27–30, 36]. Consequently, the feeding site initial (FS_i), a cell that is usually a pericycle cell, fuses with neighboring cells. The process occurs when the cell walls dissolve and the cytoplasm of adjacent cells (e.g., cortex) merges with the feeding site initial. Cell fusion, thus, results in the formation of a syncytium. Syncytial cells continue to develop in compatible roots into sites from which *H. glycines* feed (Figure 1) [27–30]. Conversely, syncytial cells of incompatible roots collapse four to five days post infection (dpi) and the nematodes die [27, 28, 30].

Understanding the localized resistance reaction at the site of infection may also lead to better measures to control *H. glycines* parasitism. The problem, however, has been in isolating these cells to some amount of homogeneity for expression analysis. Hand dissections have been performed to obtain giant cells from galls induced by the root knot nematode (*Meloidogyne incognita*) during a compatible interaction in tomato (*Lycopersicon esculentum*) [37]. The experiments permitted the isolation of cDNA from those cells [37]. However, relatively few of them turned out to be gall specific [38]. The experiments, nonetheless, demonstrated the efficacy of the approach in isolating RNA from those cell types. Unfortunately, it is not possible to use this method to study syncytium formation during *H. glycines* infection.

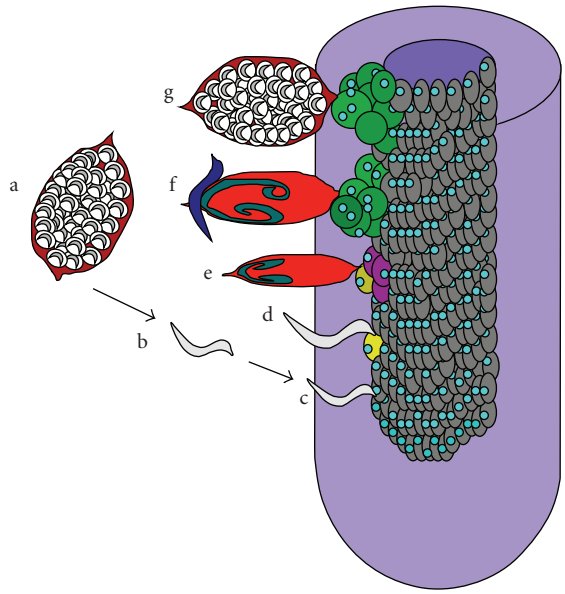

Figure 1: Life cycle of *H. glycines*. Cysts, encasing the eggs, are able to remain dormant in the soil for years. At some point, the eggs hatch. The second-stage juveniles (J2s) migrate toward the root and burrow into it. The infective J2s (i-J2s) then migrate toward the root stele. A stylet emerges from the anterior end of the nematode. The nematode selects a pericycle cell or neighboring root cell, for its feeding site. The i-J2 then presumably releases substances that then cause major changes in the physiology of the root cell. Those root cells (yellow) subsequently fuse with neighboring cells (light blue), producing a common cytoplasm. The repeated cell fusion events produces a syncytium (orange) that contains approximately 200 merged root cells and serves as the *H. glycines* feeding site. After the establishment of the syncytium, male nematodes feed for several days. Feeding proceeds until the end of their J3 stage. Meanwhile, the males become sedentary. Subsequently, the males stop feeding, followed by a molt into vermiform J4 males. The males burrow out of the root in preparation for copulation. In contrast to the males, the females become and remain sedentary after the establishment of their feeding site. The female nematodes then increase in size while undergoing both J3 and J4 molts. The J4s then mature, becoming adult feeding females. Ultimately, the female develops into the cyst that encases the eggs. (a) Cysts (dark red) with eggs (white) hatch. (b) Second-stage juveniles (J2) (gray) hatch and migrate toward the root. (c) The J2 nematodes burrow into the root and migrate toward the root stele (dark gray). (d) Feeding site selection (yellow). (e) i-J2 nematodes molt into J3 and then J4. The female is shown here in red. During this time, the original feeding site (yellow) is incorporating adjacent cells (magenta) via cell wall degradation and fusion events. Meanwhile, the male discontinues feeding at the end of its J3 stage. (f) The male and female J4 nematodes mature into adults. By this time, the feeding site has matured into a syncytium (green) as shown here where the female is actively feeding. The vermiform male (blue) migrates out of the root and subsequently copulates with the female (red). (g) After ~30 days, the female is clearly visible externally because its body emerges from the root tissue. The figure is adapted from Klink et al. [11].

Laser capture microdissection (LCM) is an alternative means that affords a high degree of precision and accuracy to isolate homogeneous cell populations that are otherwise recalcitrant to their isolation [39–42]. The method has proven to be especially valuable to study the development of the syncytium during *G. max* infection by *H. glycines* during a compatible and incompatible reaction [26, 33, 43, 44] because *H. glycines* can be used as an in situ physical marker for the syncytium. Microarray analysis studying gene expression of the syncytium has allowed for the identification of genes that exhibit differential expression in these cell types [26, 33]. However, it was unclear whether the true diversity of gene expression was being revealed by the differential expression methodology.

In the analysis presented here, DCM was used to compare detection calls made between the different cell types involved in the formation of the syncytium using samples isolated by LCM. The DCM was used to compare how the cell types under investigation (e.g., the syncytium) differed from the cell type(s) from which they originated (e.g., pericycle). Using a comparative analysis aided by customized computer scripts, a broader understanding was obtained of the differences between (1) syncytia and pericycle cells, (2) syncytia undergoing incompatible and compatible reactions, and (3) syncytia at different points of their development during a compatible reaction as they mature into a functional feeding site.

2. Materials and Methods

2.1. Female Index. The *H. glycines*$_{[NL1\text{-}RHg]}$ population used in the analyses presented here has been used extensively as race 3 for analyses requiring susceptible reactions in *G. max* genotype Kent (*G. max*$_{[Kent]}$) [22, 23, 31–33, 43, 45] and resistant reactions in *G. max*$_{[PI\ 548402/Peking]}$ [25, 26, 31, 33, 46]. For a description of the 16 nematode races and the HG-type test, please refer to Niblack et al. [35]. The HG-type test is derived from the original Index of

Parasitism test [47]. The determination of the HG-type is based on the performance of the nematode race to infect indicator lines. The indicator lines are *G. max* genotypes (including *G. max*$_{[PI\ 548402/Peking]}$) having varying ability to resist infection by the 16 known races of *H. glycines*. Based on the accepted variation of infection by *H. glycines* on the different indicator lines, an HG-type is given to an unknown sample. The numerous *G. max* genotypes are named by an accepted plant introduction (PI) classification scheme. The indicator lines now used in the HG-type test are *G. max*$_{[PI\ 88788]}$, *G. max*$_{[PI\ 548402/Peking]}$, *G. max*$_{[PI\ 90763]}$, *G. max*$_{[Pickett]}$, *G. max*$_{[PI\ 437654]}$ (*G. max*$_{[Hartwig]}$), *G. max*$_{[PI\ 89772]}$, *G. max*$_{[PI\ 548316]}$ (*G. max*$_{[Cloud]}$), *G. max*$_{[PI\ 209332]}$, and *G. max*$_{[PI\ 438489B]}$. Of note, *G. max*$_{[PI\ 438489B]}$ was added to the HG-type test to allow a more accurate test because it was classified as being resistant to five *H. glycines* races (1, 2, 3, 5, and 14) in the greenhouse [48]. The HG-type test is based off of the presence of an expected number of females, given as a proportion, which will develop on each indicator line. The number is called the female index (FI). The FI is the number of mature females that develop on a test genotype divided by the number of females that develop on a known susceptible genotype (i.e., *G. max*$_{[Lee]}$ and/or *G. max*$_{[Essex]}$) multiplied by 100. According to the original Index of Parasitism [47] any genotype with a female number less than 10% of the number determined on *G. max*$_{[Lee]}$ would be considered resistant (−) and any number above 10% would be susceptible (+). The HG-type test as determined by Niblack et al. [35] has changed the Index of Parasitism test [47] and improved race test [34] to include several other categories. Now, the FI categories for the HG-type test are Highly Resistant, FI: 0%–9%; Resistant, FI: 10%–24%; Moderately Resistant, FI: 25%–39%; Low Resistance, FI: 40%–59%; and No Effective Resistance, FI: >60%. The HG-type test for *H. glycines*$_{[NL1\text{-}RHg]}$ was determined independently in the lab of Dr. Terry Niblack (Department of Crop Sciences, University of Illinois) [11, 25] during June-July, 2007 using the published methods of Niblack et al. [35]. The performance of *H. glycines*$_{[NL1\text{-}RHg]}$ on those indicator lines was compared to the susceptible genotypes *G. max*$_{[Lee]}$ and *G. max*$_{[Essex]}$. An FI of 0 (0%) was found for *H. glycines*$_{[NL1\text{-}RHg]}$ on *G. max*$_{[PI\ 548402/Peking]}$. Thus, the HG-type test determined that *G. max*$_{[PI\ 548402/Peking]}$ is considered highly resistant to *H. glycines*$_{[NL1\text{-}RHg]}$. Based on the infectivity of *H. glycines*$_{[NL1\text{-}RHg]}$ on the indicator lines, the HG-type test also determined that *H. glycines*$_{[NL1\text{-}RHg]}$ is race 3, as previously published [22, 23, 31, 43, 45, 49]. *H. glycines*$_{[NL1\text{-}RHg]}$ (incompatible) is HG-type 7 (*H. glycines*$_{[NL1\text{-}RHg/HG\text{-}type\ 7]}$). The reaction of *H. glycines*$_{[TN8]}$ (HG-type 1.3.6.7 [race 14]) (*H. glycines*$_{[TN8/HG\text{-}type\ 1.3.6.7]}$) (compatible) on *G. max*$_{[PI\ 548402/Peking]}$ is a susceptible reaction [50].

2.1.1. Plant and Nematode Procurement. The methods have been published previously [26, 33]. Briefly, plant and nematode materials were grown at the United States Department of Agriculture, Soybean Genomics and Improvement Laboratory (SGIL). A single *G. max* genotype (*G. max*$_{[PI\ 548402/Peking]}$) was used in the experiments to obtain both incompatible and compatible reactions by the use of two different populations of *H. glycines, H. glycines*$_{[NL1\text{-}RHg/HG\text{-}type\ 7]}$ and *H. glycines*$_{[TN8/HG\text{-}type\ 1.3.6.7]}$. The *H. glycines* populations were maintained in the greenhouse using the moisture replacement system (MRS) [51].

The origin of *H. glycines*$_{[TN8/HG\text{-}type\ 1.3.6.7]}$ was by selection of a single-cyst descent on *G. max*$_{[PI\ 90763]}$ [50]. Originally, *H. glycines*$_{[TN8/HG\text{-}type\ 1.3.6.7]}$ was maintained on the *G. max*$_{[PI\ 90763]}$ genotype according to Niblack et al. [50]. The *H. glycines*$_{[TN8/HG\text{-}type\ 1.3.6.7]}$-infected *G. max* plants were maintained in sterilized field sand medium in 1liter containers. The containers were suspended in a 27°C water bath. Fertilization of *G. max* was done with Peter's soluble 20-20-20 nutrients (The Scotts Company; Marysville, OH). Transfer of *H. glycines*$_{[TN8/HG\text{-}type\ 1.3.6.7]}$ to a new host was performed routinely on a 30–40 day basis. The *H. glycines*$_{[TN8/HG\text{-}type\ 1.3.6.7]}$ population is maintained at SGIL on the susceptible *G. max*$_{[Kent]}$. The *H. glycines*$_{[NL1\text{-}RHg/HG\text{-}type\ 7]}$ population has been maintained on *G. max*$_{[Kent]}$ at SGIL. The *H. glycines*$_{[NL1\text{-}RHg/HG\text{-}type\ 7]}$ population has been used extensively for analyses requiring susceptible reactions in *G. max*$_{[Kent]}$ [22, 23, 43] and resistant reactions in *G. max*$_{[PI\ 548402/Peking]}$ [25, 26, 31, 33, 46]. Thus, in side-by-side experiments, *H. glycines*$_{[TN8/HG\text{-}type\ 1.3.6.7]}$ and *H. glycines*$_{[NL1\text{-}RHg/HG\text{-}type\ 7]}$ have always been exposed to the same *G. max* genotypes. The method virtually eliminated variations among the different *G. max* genotypes in influencing the experiments.

Seedlings were grown in sterilized sand in 20 × 20 × 10 cm flats for a period of one week. The plants were gently removed from the sand and rinsed with sterile water. Seedlings were placed on moistened germination paper (Anchor Paper; St. Paul, MN) inside the flats. Mature female nematodes were harvested by massaging the roots in water. Mature nematodes were collected by filtering the solution through nested 850 and 150 μm sieves. Females were further purified by sucrose flotation [45]. The females were crushed gently with a rubber stopper within a 7.5 cm diameter apparatus containing 250 μm sieves. The process released the eggs. The eggs passed through the sieve into a small plastic tray. Debris smaller than the eggs was removed. Debris removal was done by washing the debris in a 25 μm mesh sieve. The eggs were placed in a small plastic tray containing 1 cm of water. The tray was covered with plastic wrap and subsequently placed on a rotary shaker at 25 rpm. After 3 days, the second-stage juvenile nematodes (J2s) were separated from the unhatched eggs. Separation was done by passing them through a 41 μm mesh cloth. The J2s were concentrated by centrifugation in an IEC clinical centrifuge for 30 seconds at 1720 rpm to 5,000 J2/mL. The nematodes were used to infest the roots. There were 2 mL of nematode-containing solution added directly on the roots for a final concentration of 2,000 J2/root. The control mock-infested replicates received the same amount of water. The roots were covered with a moistened sheet of germination paper. The plants were placed in a 45 × 50 × 20 cm plastic tray

with a one cm of water in the bottom to add humidity. A semitransparent bag was then wrapped around the tray. The trays were then placed under fluorescent lights of 16/8 hour light/dark photoperiod. Light intensities were identical for all experiments. Infested roots were grown for three or 8 dpi. The mock-infested control samples and susceptible and resistant reactions were washed. The process removed the extraneous nematodes that had not yet penetrated the root, preventing additional nematodes from entering the root. The process ensured that tissue that was the most highly infested with nematodes was obtained. The process was then repeated, providing two independent sets of samples. Seven independent replicates were pooled to obtain each replicate for each sample type in the analysis. Thus, there are a total of 14 replicates used in the analysis. At least 50 serially sectioned syncytia were used for each of the 7 replicates. Materials for histological observation to confirm incompatible and compatible reactions were derived from these samples (see below).

2.1.2. Histology. Histological tissue processing was according to Klink et al. [26, 33, 43]. Briefly, tissue was fixed in Farmer's solution (FS) composed of 75% ethanol and 25% acetic acid v/v [43, 52]. Some replicate samples of roots used for immunohistochemical analyses were killed and fixed in 3.7% w/v paraformaldehyde (PFA) buffered with PEMP buffer (100 μM Pipes, 1 μM EGTA, 1 μM $MgCl_2$, and 4% w/v polyethylene glycol MW 8000, pH 6.8) [43, 53]. *G. max* root tissue was harvested and cut into 0.5 cm pieces. Those pieces were vacuum infiltrated with either FS or PFA at room temperature for one hour (h). Fresh fixative (FS or PFA) was then added to their respective samples. Tissue was subjected to an incubation step of 12 hours at 4°C. PFA fixed tissue was then dehydrated through 10% (v/v), 25% (v/v), 50% (v/v), 75% (v/v) ethanol : water. The remaining procedure was done identically as for FS processed tissue. Fixative was removed from the roots. Dehydration of FS-fixed tissue proceeded through a graded series of 75% (v/v), 85% (v/v), 100% (v/v), 100% (v/v) ethanol : water, 30 minutes each. Ethanol was replaced with 1 : 1 (v/v) xylene : ethanol for 30 minutes. Subsequently, three, 100% xylene incubations (30 minutes each) were done. Xylene was replaced by paraffin. The processing was done slowly by placing the specimens into a 58°C oven. The roots were infiltrated sequentially in 3 : 1 (v/v), 1 : 1 (v/v), 1 : 3 (v/v) xylene : Paraplast+ tissue embedding medium (Tyco Healthcare Group LP; Mansfield, MA) in each step for three hours. Tissue was cast and subsequently mounted for sectioning. Serial sections of roots were made on an American Optical 820 microtome (American Optical Co.; Buffalo, NY) at a section thickness of 10 μm. Sections were stained in Safranin O (Fischer Scientific) in 50% (v/v) ETOH : water and counter-stained in Fast Green FCF (Fisher Scientific). The tissue was permanently mounted in Permount (Fisher Scientific).

2.2. LCM. Slides were prepared according to Klink et al. [26]. MembraneSlides (Leica, Germany; Cat# 11505158) were placed on a slide warmer set at 40°C. DEPC-treated RNAse-free water (~0.5–1 mL) was placed onto the slide and allowed to warm. The tissues used for these analyses were obtained from the same tissue used in whole-root microarray experiments [26]. Serial sections (10 μm) from control mock-inoculated roots and roots undergoing incompatible (3 dpi) and compatible (3 and 8 dpi) reactions were prepared according to Klink et al. [26, 33, 43]. Serial sections for the independent sample types were placed directly onto the pool of DEPC-treated water. DEPC-treated water was blotted off with a sterile KimWipe after the serial sections were adequately spread. Tissue was allowed to warm on the slide warmer for an additional hour to promote tissue binding to the slide surface. Slides were deparaffinized for five minutes in xylene. The processing was followed by a two-minute incubation in 1 : 1 (v/v) xylene : ETOH. That was followed subsequently with two one-minute incubations in ETOH. Slides were then dried on the lab bench on filter paper covered with KimWipes. The slides were used immediately for LCM after the drying step was done. LCM was performed on a Leica ASLMD microscope (Leica). Microdissection cutting parameters were determined empirically for each session by examining how amenable the tissue was to LCM. However, cutting parameters for dissections performed on the 40× objective were approximately power, 55–85; speed, 2–4; specimen balance, 1–3; and offset, 40. Similar quantities of cells were obtained for each sample type for the analyses.

Tissue was collected in OptiCaps (Leica Cat. number 11505169) and subsequently washed to the bottom of the OptiCap PCR tube. The process was done by micropipetting 20 μL of XB buffer (Arcturus) onto the microdissected tissue. The cap was spun for five minutes at 500 rpm to pellet the tissue into the bottom of the Opticap. LCM tissue was ground with a micropestle. The process was done in 40 μL RNA extraction buffer (Arcturus). The RNA was extracted and subsequently processed using the PicoPure RNA Isolation Kit (Arcturus). The process was done according to the manufacturer's instructions. A DNAse treatment was added, just before the second column wash, using DNAfree (Ambion; Austin, TX). RNA quality and yield were determined. The processing was done using the RNA 6000 Pico Assay (Agilent Technologies; Palo Alto, CA) using the Agilent 2100 Bioanalyzer according to the manufacturer's instructions. RNA amplification of LCM samples was performed with the GeneChip Two-Cycle cDNA Synthesis Kit (Affymetrix; Santa Clara, CA: Cat. number 900432). Probe preparation and hybridizations were performed according to Affymetrix guidelines at the Laboratory of Molecular Technology, SAIC-Frederick, Inc., National Cancer Institute at Frederick, Frederick, MD 21701, USA.

2.3. Microarray Analyses and G. max Probe Set Annotations. The GeneChip Soybean Genome Array (Affymetrix; Cat. number 900526) containing 37,744 *G. max* transcripts (35,611 transcripts) was used for the microarray analyses. Details of the GeneChip soybean genome array can be obtained (http://www.affymetrix.com/index.affx). Annotations were made by comparison to the *Arabidopsis thaliana* gene ontology (GO) database [54] based on their best match obtained by BLAST searches [55]. They were updated (2009).

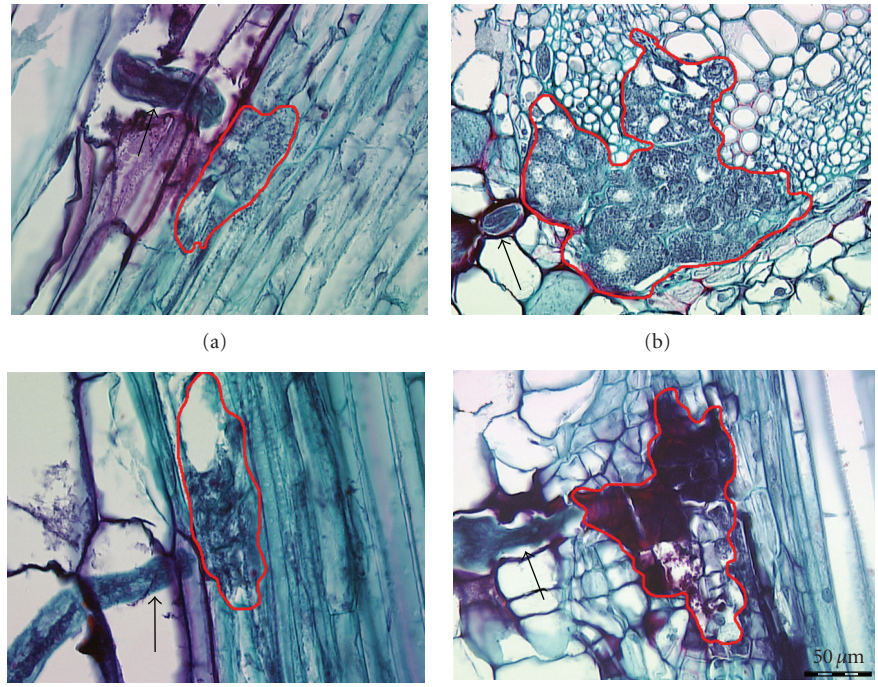

FIGURE 2: *G. max*[PI 548402/Peking] seedlings were inoculated with incompatible or compatible *H. glycines* J2 nematodes. Roots were harvested and prepared for histological observation to confirm the establishment of feeding sites at three and 8 dpi. (a) 3 dpi *G. max*[PI 548402/Peking] infected with a compatible nematode, black arrowhead; area encircled in red, syncytial cell. (b) 8 dpi *G. max*[PI 548402/Peking] infected with a compatible nematode, black arrowhead; area encircled in red, syncytial cell. (c) 3 dpi *G. max*[PI 548402/Peking] infected with an incompatible nematode, black arrowhead; area encircled in red, syncytial cell. (d) 8 dpi *G. max*[PI 548402/Peking] infected with an incompatible nematode, black arrowhead; area encircled in red, syncytial cell. Bar = 50 μm.

All microarray hybridizations were performed at the Laboratory of Molecular Technology, SAIC-Frederick, National Cancer Institute at Frederick, Frederick, MD 21701, USA. Local normalization was used. The presence or absence of a particular probe set's (gene's) transcript on a single array was determined using the Bioconductor implementation of the standard Affymetrix DCM. In summary, the DCM consists of four steps: (1) removal of saturated probes, (2) calculation of discrimination scores, (3) *P*-value calculation using the Wilcoxon's rank test, and (4) making the detection (present/marginal/absent). Ultimately, the algorithm determines if the presence of a probe set's transcript is provably different from zero (present (P)), uncertain (marginal (M)), or not provably different from zero (absent (A)). Details of the standard Affymetrix DCM can be found in their *Statistical Algorithms Description Document* (http://www.affymetrix.com/support/technical/whitepapers/sadd_whitepaper.pdf.). For a particular condition (e.g., 3 dpi syncytia during the incompatible response), a probe set was considered present only if it was present on both replicate microarrays corresponding to that condition. Otherwise, it was considered to be absent. All original data sets, the normalized data sets, statistics, and data supplemental to each table and figure are available at the MAIME compliant [http://bioinformatics.towson.edu/SGMD3] [56].

3. Results

3.1. Histological Analysis of Incompatible and Compatible Responses in the Whole Root. Morphological and anatomical details of compatible and incompatible disease responses by *G. max* to *H. glycines* infection have been published previously [27–29, 36, 57–61]. Infection during the first 8 dpi (Figure 2) was focused on for this analysis because syncytial cells complete the incompatible reaction by 8 dpi under the experimental conditions in *G. max*[PI 548402/Peking]. During a compatible reaction, nematodes have selected and are establishing feeding sites by 3 dpi (Figure 2(a)) that are continuing to develop by 8 dpi (Figure 2(b)). During an incompatible reaction, nematodes have also selected and are establishing feeding sites at 3 dpi (Figure 2(c)). However, during an incompatible reaction, syncytial cells collapse by 8 dpi (Figure 2(d)). Syncytial cells (Figure 3(a)) for the various analyses were collected by LCM (Figure 3(b)).

3.2. The Use of Detection Calls to Identify Genes Present in Syncytium Samples. The DCM was used to make a comparative analysis of the probe sets measuring the presence of a transcript (present transcript) within LCM-derived cell samples. The analyses would allow (1) the determination of the total number of present transcripts, (2) the determination of the

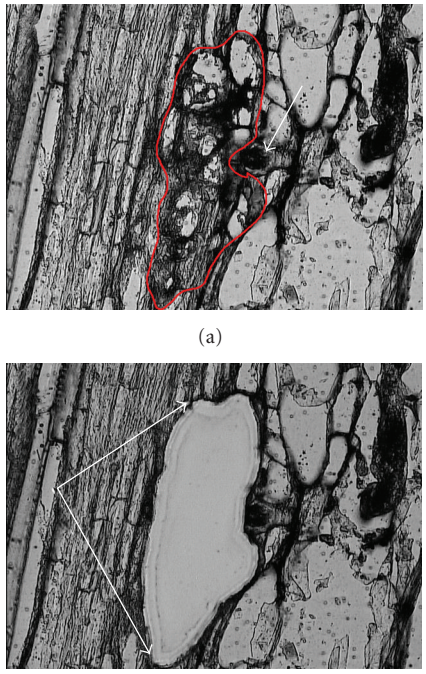

(a)

(b)

Figure 3: Microdissection of a syncytial cell. (a) A 3 dpi time point syncytial cell (area encircled in red) prior to microdissection was identified by their proximity to *H. glycines* (white arrow). (b) The same syncytial cell section from (a) after microdissection, microdissected syncytial cell (area between white arrows).

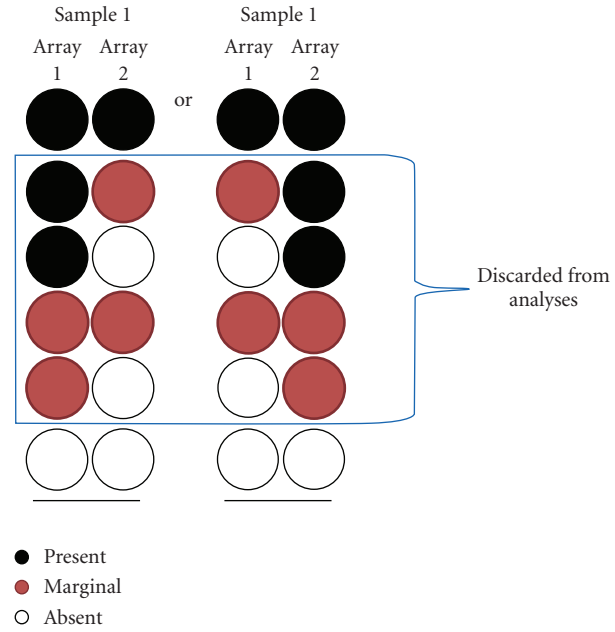

Figure 4: Determination of probe sets to be used in the analysis. Sample 1: the particular sample under investigation (e.g., 3 dpi incompatible syncytia). Array 1: first array analyzed by DCM; Array 2: second array analyzed by DCM for a particular sample type. The word *or* refers to the order that the probe set measures present/marginal/absent on array 1 or array 2.

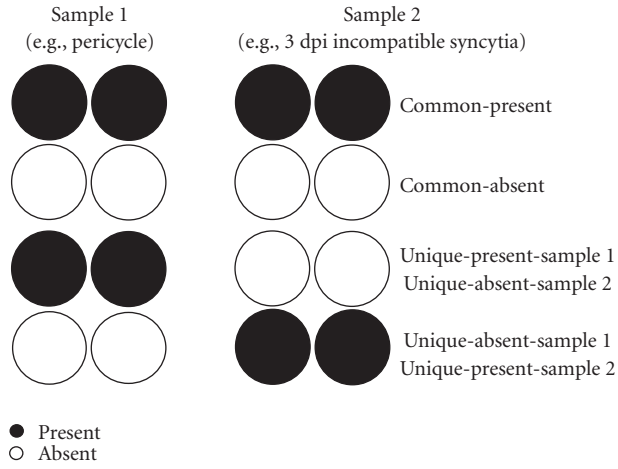

Figure 5: Diagram of the comparative analysis of DCM between two sample types. The probe sets with like measurements are common. The probe sets with dissimilar measurements are unique.

numbers of present transcripts within a sample, and (3) a comparison of the present transcripts between the different sample types while estimating the differences between those samples (4) the identification of whether transcripts that are common between the two sample types under comparison had been identified in a prior differential expression analysis [26]. Only probe sets that measured detection on both arrays for a particular sample type (Figure 4) were evaluated further (see below).

While detection calls are generally used for single array analyses, the DCM presented here used two arrays for each sample type in a comparison. Thus, for a particular comparison between cell types, four arrays were taken into consideration. Detection calls were analyzed for each of the two arrays for each sample type (e.g., pericycle). Detection calls were made for each of the two arrays independently to determine if the probe sets were consistently measuring present or absent for a particular sample type. For example, the probe set had to obtain a like measurement (e.g., present/present; absent/absent) for each of the two arrays for each sample type to be considered for subsequent analyses (Figure 4). The arrays that measured present on both arrays within a sample type are considered present. The arrays that measured absent on both arrays within a sample type are considered absent (Figure 4). The probe sets that failed to produce like measurements (e.g., any combination of present/absent; present/marginal for the two arrays) and those that measured marginal amounts of a transcript for a particular probe set on each of the two arrays (e.g., marginal/marginal) were excluded from the analysis (Figure 4). The resulting probe sets used in the subsequent analyses were measuring present/present detection calls for each of the two arrays for a particular sample type (e.g., 3 dpi incompatible syncytia).

Comparisons were made between the different sample types (e.g., 3 dpi incompatible syncytia versus pericycle). In those comparisons, four arrays would be compared (Figure 5). Probe sets that measured detectable amounts

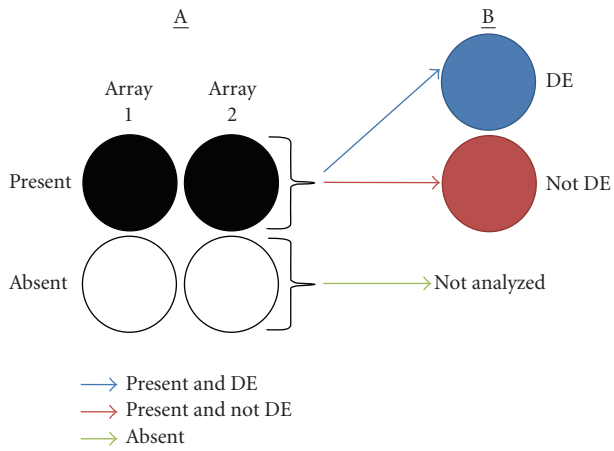

Figure 6: A diagram of the comparative analysis between the (A) DCM and (B) differential expression analyses [26]. DE: differentially expressed.

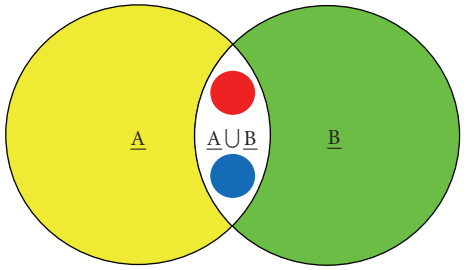

Figure 7: Comparative analysis of DCM and differential expression analyses. Pools A and B are different sample types. Analyses have identified genes that are unique to A (yellow), genes that are unique to B (green), and genes common to both pools (A ∪ B). Only genes that are present in both A and B can be used for differential expression analyses. The red circle represents the genes that are present in both pools and are also differentially expressed, measuring induced gene activity. The blue circle represents the genes that are present in both pools that are differentially expressed, measuring suppressed gene activity. The remaining genes (white) are present in both samples (common) but are not differentially expressed.

of a transcript on the four arrays under comparison were considered common and present between two sample types (e.g., pericycle and 3 dpi incompatible syncytia-common). The probe sets measuring absent on the four arrays (common and absent), although potentially interesting, were not taken into consideration in this analysis. The samples whose probe sets measured present for both arrays but only in one of the two sample types would be considered present and unique for a particular sample type (e.g., pericycle-unique or 3 dpi incompatible syncytia-unique) (Figure 5). Probe sets that measure detectable amounts of gene activity in both sample types can either be differentially expressed or not differentially expressed (Figure 6). The differential expression calls used in some of the comparative analyses had been presented previously [26]. The DCM analysis presented here is employed as a different way of examining the data with the goal of identifying genes at low thresholds of expression that are missed in differential expression analyses. More importantly, DCM is also a way of identifying genes that may be expressed at high thresholds in one sample type and are undetectable in a second sample type used for comparative purposes in a differential expression analysis. In cases like these, statistical analyses cannot be done because no expression data is available for the second sample type and thus the probe set is excluded from the differential expression analysis. Therefore, probe sets that measured detectable amounts of a transcript uniquely in one sample type (e.g., unique-present) (Figure 5) cannot measure differential expression (Figure 6). An example of genes identified in a comparative analysis of two hypothetical gene pools (Figure 7) illustrates the different gene categories investigated in the analysis (Figure 8). As illustrated, all genes that are identified as differentially expressed had to be present in each gene pool (Figure 7). It became clear from the analysis that many genes that were unique to a specific sample type (e.g., A or B) were being excluded from the differential expression analysis because the probe sets measured detectable levels of gene activity only in one of the two sample types (Figure 7). The probe sets that match this criterion, A or B and not A U B, became the focus of the analysis (Figure 8).

3.3. The DCM Identifies Many Genes Expressed in the Experimental Cell Types. The DCM identified a total of 13,291 transcripts as being present between the pericycle, 3 dpi incompatible syncytium, 3 dpi compatible syncytium, and the 8 dpi compatible syncytium samples. Direct comparisons were made between each of the sample types. The analyses focused on two types of transcripts that were determined to be present. The transcript types are (1) unique and (2) common. Unique transcripts were defined as those that were present and found in only one of the two sample types being compared. Common transcripts were defined as those that were present and overlap between the two sample types being compared. Data from five of the comparisons (Figures 8(a), 8(c), 8(e), 8(g), 8(i)) are presented as Venn diagrams. The annotated probe sets were divided into seven subcategories (histograms) per functional category (Figures 8(b), 8(d), 8(f), 8(h), 8(j) (A–R—see figure legends)), based on the particular comparison being made (see below). The comparison in Figure 8(g), presented as a Venn diagram, was divided into eight subcategories (histograms) per functional category (see below).

3.4. 3 dpi Syncytia Undergoing an Incompatible Reaction. The DCM was used to compare present transcripts (genes) within the 3 dpi microdissected syncytia undergoing an incompatible reaction to the pericycle sample (Figures 8(a) and 8(b)). A total of 3,908 genes were present in these two samples. The DCM identified 1,966 genes that were present and unique to the pericycle sample (Figures 8(a)(see Table 1 in Supplementary Material available online at 10.1155/2010/491217)). Further analysis identified 1,002 genes that were present

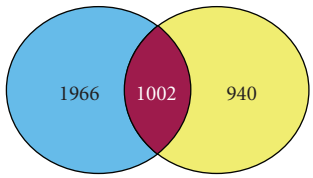

(a)

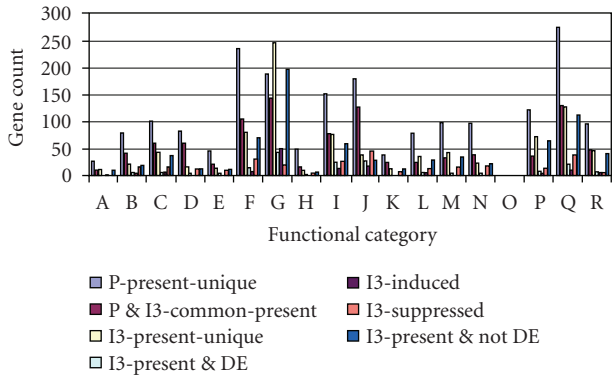

(b)

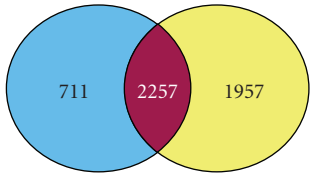

(c)

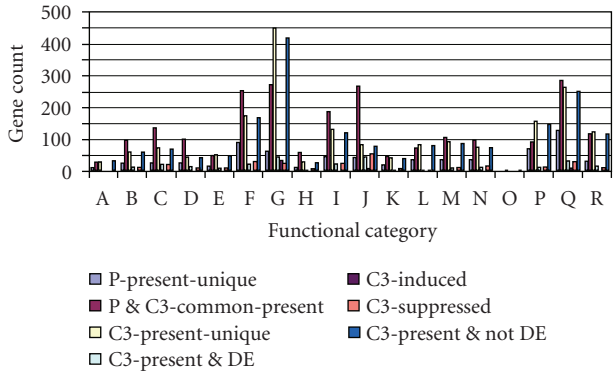

(d)

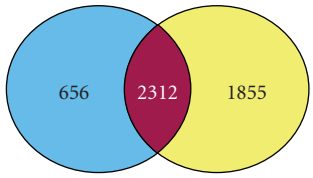

(e)

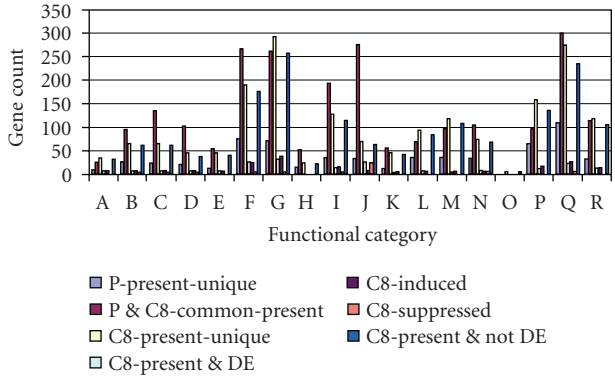

(f)

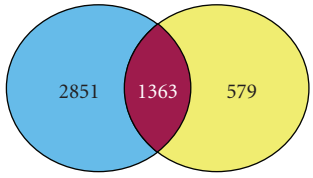

(g)

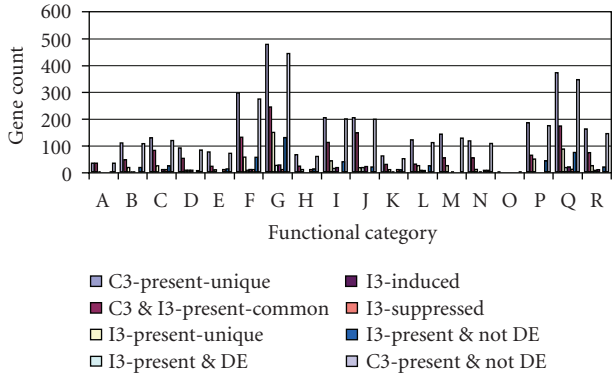

(h)

Figure 8: Continued.

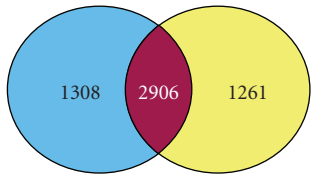

(i)

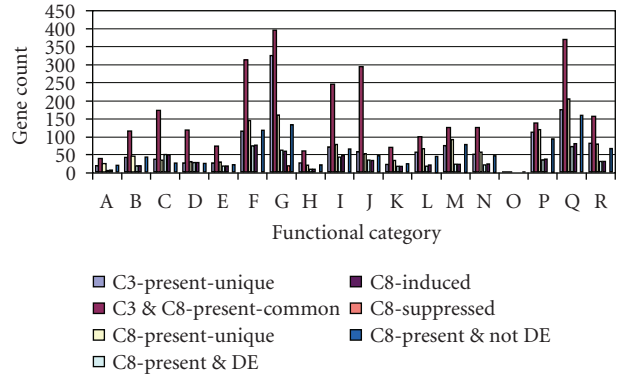

(j)

Figure 8: Detection calls. (a, c, e, g, i) Gene counts per sample. (b, d, f, h, j) Functional categories for the histograms. P: pericycle; I3: incompatible syncytium-3 dpi; C3: compatible syncytium 3 dpi; C8: compatible syncytium-8 dpi; DE: differentially expressed. The functional categories are as follows: A: Cell Growth & Division; B: Cell Structure; C: Disease & Defense; D: Energy; E: Intracellular Traffic; F: Metabolism; G: No Homology to Known Proteins; H: Post-Transcription; I: Protein Destination & Storage; J: Protein Synthesis; K: Secondary Metabolism; L: Signal Transduction; M: Transcription; N: Transporter; O: Transposon; P: Unclassified-Hypothetical Protein NOT Supported by cDNA; Q: Unclassified-Hypothetical Protein Supported by cDNA; R: Unclassified-Protein with Unknown Function. (a) Venn diagram depicting P versus I3. The three portions of the Venn diagram show transcripts for P-present-unique; common-present; I3-present-unique. (b) Functional categorization depicting P versus I3. The seven histograms (per functional category) are P-present-unique; common-present; I3-present-unique. The remaining four transcript identifications represent comparisons between those that measured DE [26] and those that were present: I3-present & DE; I3-DE-induced; I3 dpi-DE-suppressed; I3-present & not DE. (c) Venn diagram depicting P versus C3. The three portions of the Venn diagram show transcripts for P-present-unique; common-present; C3-present-unique. (d) Functional categorization depicting P versus C3. The seven histograms (per functional category) are P-present-unique; common-present; C3-present-unique. The remaining four transcript identifications represent comparisons between those that measured DE [26] and those that were present: C3-present & DE; C3-DE-induced; C3-DE-suppressed; C3-present & not DE. (e) Venn diagram depicting P versus C8. The three portions of the Venn diagram show transcripts for P-present-unique; common-present; C8 present-unique. (f) Functional categorization depicting P versus C8. The seven histograms (per functional category) are P-present-unique; common-present; C8-present-unique. The remaining four transcript identifications represent comparisons between those that measured DE [26] and those that were present: C8-present & DE; C8-DE-induced; C8-DE-suppressed; C8-present & not DE. (g) Venn diagram depicting C3 versus I3. The three portions of the Venn diagram show transcripts for C3-present-unique; common-present; I3-present-unique. (h) Functional categorization depicting C3 versus I3. The eight histograms (per functional category) are C3-present-unique; common-present; I3-present-unique. The remaining five transcript identifications represent comparisons between those that measured DE [26] and those that were present: I3-present & DE; I3-DE-induced; I3-DE-suppressed; I3-present & not DE; C3-present & not DE. (i) Venn diagram depicting C3 versus C8. The three portions of the Venn diagram show transcripts for C3-present-unique; common-present; C8-present-unique. (j) Functional categorization depicting C3 versus C8. The seven histograms (per functional category) are C3-present-unique; common-present; C8-present-unique. The remaining four transcript identifications represent comparisons between those that measured DE [26] and those that were present: C8-present & DE; C8-DE-induced; I3-DE-suppressed; C8-present & not DE.

and common between the pericycle and 3 dpi incompatible syncytium sample (Figure 8(a) (supplementary Table 2)). Only the genes that are present and common can be used for differential expression analyses because expression data was available for each sample type. An analysis identified 940 genes present and unique to the 3 dpi incompatible syncytium sample (Figure 8(a) (supplementary Table 3)). Therefore, in the analysis presented here, a total of 1,942 genes within 3 dpi incompatible syncytial cell samples were present. Customized computer scripts were written to make seven comparisons of those genes. Some of these comparisons were made to genes identified previously as being differentially expressed between the two cell types under investigation [26]. A histogram of the functional categorizations of the 940 genes present and unique to the 3 dpi incompatible syncytium sample is presented (Figure 8(b)). Selected gene lists comprising the (1) Disease and Defense, (2) Signaling, and (3) Transcription categories are provided (Table 1 (supplementary Table 3)).

3.5. 3 dpi Syncytia Undergoing a Compatible Reaction. The DCM was used to compare genes within the 3 dpi microdissected syncytia undergoing a compatible reaction to the pericycle sample (Figures 8(c) and 8(d)). A total of 4,925 genes were present in these two samples. From these analyses, 711 genes were identified that were present and unique to the pericycle sample (Figure 8(c) (supplementary Table 4)). Further analysis identified 2,257 genes that were present and common between the pericycle and 3 dpi compatible syncytium sample (Figure 8(c) (supplementary Table 5)). Only these genes could be used for differential expression analyses because expression data was available for each

Table 1: Select genes that were unique to the 3 dpi syncytia undergoing an incompatible reaction but that were not differentially expressed as compared to a pericycle control sample (Figure 8(b)) comprising the Disease and Defense, Signaling, and Transcription categories.

I-3 dpi			
Probe set ID	Public ID	Avg *P*-value	Gene
Disease & defense			
Gma.4886.2.S1_at	AW234624	0.005201937	haem peroxidase
GmaAffx.69994.1.S1_at	CD417025	0.017952293	phosphate-responsive protein (phi-1)
Gma.8449.1.S1_s_at	AF002258.1	0.019563038	CoA ligase 4
GmaAffx.14986.1.S1_at	BE657889	0.020669698	phosphate-responsive protein (phi-1)
GmaAffx.93611.1.S1_s_at	CF809336	0.034312943	disease resistance response protein (DRRG49-C)
Signal transduction			
Gma.1965.1.S1_x_at	L01432.1	0.005201937	calmodulin (SCaM-3)
GmaAffx.50980.1.S1_x_at	BE823095	0.006003594	protein phosphatase 2C (PP2C)
Gma.11041.1.S1_at	BI970555	0.006660588	Pti1-like kinase-like
GmaAffx.33721.1.S1_at	BI967195	0.006660588	protein kinase
Gma.6290.1.S1_at	AW311265	0.007290178	BOTRYTIS-INDUCED KINASE1 (BIK1)
Gma.13604.1.S1_at	CD401537	0.011411572	protein kinase-like
Gma.9902.1.A1_at	AW395328	0.011756578	FUSCA 5 MAP kinase kinase (FUS5)
GmaAffx.56323.1.S1_at	BU764214	0.01212639	protein kinase
Gma.5162.1.A1_at	BI971156	0.013412317	Curculin-like (mannose-binding) protein kinase
Gma.4455.3.S1_at	CB063632	0.014076915	PROTEIN KINASE 2B (APK2B)
GmaAffx.21787.1.A1_at	AW348555	0.015096504	leucine-rich repeat transmembrane protein kinase (CLAVATA1)
GmaAffx.66511.1.S1_at	AW350917	0.019563038	calcium and calmodulin-dependent protein kinase (ATCDPK1)
GmaAffx.34312.1.S1_at	AI965735	0.023684433	protein phosphatase 2C (PP2C)
GmaAffx.64402.1.S1_at	AW317282	0.025399823	leucine-rich repeat
Gma.4801.1.S1_s_at	BU548608	0.028086024	protein phosphatase 1 (PP1)
Gma.11291.1.S1_at	AW351207	0.028086024	inositol 1,3,4-trisphosphate 5/6-kinase
GmaAffx.73451.1.S1_at	BG046889	0.034312943	CALMODULIN-RELATED PROTEIN 2
Transcription			
Gma.7212.1.S1_at	BE658102	0.005553929	SUPPRESSOR OF FRIGIDA4 (SUF4)
GmaAffx.67609.1.S1_at	BG551013	0.009290923	SAR DNA-binding protein-1
Gma.4165.1.S1_at	BI969143	0.015813164	homeodomain-related
Gma.4164.1.S1_at	BI968666	0.016772715	MYB transcription factor (MYB112)
GmaAffx.1165.1.S1_at	BI425542	0.01738237	jasmonate-responsive promoter element
Gma.15724.2.S1_at	AW350291	0.018668953	CCR4 associated factor 1-related protein
Gma.1772.1.S1_at	CD406036	0.020753499	transcription factor IIA (TFIIA)
GmaAffx.52970.1.S1_at	BU548330	0.021323422	zinc finger (DHHC type) family protein

Table 1: Continued.

I-3 dpi			
Probe set ID	Public ID	Avg *P*-value	Gene
Transcription			
Gma.4560.1.S1_at	CD393558	0.022830045	TINY-like
Gma.12330.2.S1_s_at	BI972758	0.027055562	pathogenesis-related transcriptional factor
Gma.6838.1.S1_at	AW349633	0.027055562	NIM1-like protein 1 (NPR-1)
Gma.13614.1.A1_at	CD402000	0.034312943	zinc finger protein

sample type. The detection call analysis identified 1,957 genes present and unique to the 3 dpi compatible syncytium sample (Figure 8) (supplementary Table 6)). Therefore, in the analysis presented here, a total of 4,214 genes were present within 3 dpi compatible syncytial cell samples. A histogram of the functional categorizations of the 1957 genes present and unique to the 3 dpi compatible syncytium sample described in this section is presented (Figure 8(d)). Selected gene lists comprising the (1) Disease and Defense, (2) Signaling, and (3) Transcription categories are provided (Table 2 (supplementary Table 6)).

3.6. 8 dpi Syncytia Undergoing a Compatible Reaction. The DCM was used to compare genes within the 8 dpi microdissected syncytia undergoing a compatible reaction to the pericycle sample (Figures 8(e) and 8(f)). A total of 4,823 genes were present in these two samples. From these analyses, 656 genes that were present and unique to the pericycle sample were identified (Figure 8(e) (supplementary Table 7)). Further analysis identified 2,312 genes that were present and common between the pericycle and 8 dpi compatible syncytium sample (Figure 8(e) (supplementary Table 8)). Only these genes could be used for differential expression analyses because expression data was available for each sample type. The detection call analysis identified 1,855 genes present and unique to the 8 dpi compatible syncytium sample (Figure 8(e) (supplementary Table 9)). Therefore, in the analysis presented here, a total of 4,167 genes within 8 dpi compatible syncytial cell samples were present. A histogram of the functional categorizations of the 4,167 genes present and unique to the 8 dpi compatible syncytium sample described in this section is presented (Figure 8(f)). Selected gene lists comprising the (1) Disease and Defense, (2) Signaling, and (3) Transcription categories are provided (Table 3 (supplementary Table 9)).

3.7. Direct Comparison: 3 dpi Incompatible versus 3 dpi Compatible Syncytia. The DCM was used to compare genes within the 3 dpi microdissected syncytia undergoing an incompatible reaction directly to the 3 dpi syncytia undergoing a compatible reaction (Figures 8(g) and 8(h)). A total of 4,793 genes were present in these two samples. From these analyses, 2,851 genes were identified that were present and unique to the 3 dpi compatible syncytium sample (Figure 8(g) (supplementary Table 10)). Further analysis identified 1,363 genes that were present and common between the 3 dpi syncytia undergoing compatible and incompatible reactions (Figure 8(g) (supplementary Table 11)). Only these genes could be used for differential expression analyses because expression data was available for each sample type. The detection call analysis identified 579 genes present and unique to the 3 dpi incompatible syncytium sample (Figure 8(g) (supplementary Table 12)). A histogram of the functional categorizations of the 579 genes present and unique to the 3 dpi incompatible syncytium (as directly compared to the present and unique to the 3 dpi compatible syncytium sample genes) described in this section is presented (Figure 8(h)). Selected gene lists for the incompatible syncytium (Table 4) and compatible syncytium (Table 5) comprising the (1) Disease and Defense, (2) Signaling, and (3) Transcription categories are provided.

3.8. Direct Comparison: 8 dpi Compatible versus 3 dpi Compatible Syncytia. The DCM was used to compare genes within the 8 dpi microdissected syncytia undergoing a compatible reaction to the 3 dpi syncytia undergoing a compatible reaction (Figures 8(i) and 8(j)). A total of 5,475 genes were present in these two samples. From these analyses, 1,308 genes were identified that were present and unique to the 3 dpi compatible syncytium sample (Figure 8(i) (supplementary Table 13)). The detection call analysis identified 2,906 genes that were present and common between the three and 8 dpi syncytia undergoing compatible reactions (Figure 8(i) (supplementary Table 14)). Only these genes could be used for differential expression analyses because expression data was available for each sample type. Further analysis identified 1,261 genes present and unique to the 8 dpi compatible syncytium sample (Figure 8(i) (supplementary Table 15)). A histogram of the functional categorizations of the 1,261 genes present and unique to the 8 dpi compatible syncytium sample (as directly compared to the present and unique to the 3 dpi compatible syncytium sample genes) described in this section is presented (Figure 8(j)). Selected gene lists comprising the (1) Disease and Defense, (2) Signaling, and (3) Transcription categories are provided (Table 6 (supplementary Table 15)).

4. Discussion

Microarray experiments typically rely on differential expression analysis methods to identify differences in relative levels

Table 2: Select genes that were unique to the 3 dpi syncytia undergoing a compatible reaction but that were not differentially expressed as compared to a pericycle control sample (Figure 8(d)) comprising the Disease and Defense, Signaling, and Transcription categories.

C-3 dpi			
Probe set ID	Public ID	Avg *P*-value	Gene
Disease & defense			
Gma.3749.1.S1_at	CD392491	0.002923594	heat shock protein 70 precursor
GmaAffx.90134.1.S1_s_at	CF805859	0.008396837	purple acid phosphatase-like protein
GmaAffx.78614.1.S1_at	BQ611991	0.008396837	Suppressor-of-White-APricot/surp domain-containing protein
Gma.13217.1.S1_at	CD391191	0.011756578	wound-responsive protein-related
GmaAffx.11893.1.A1_at	CD414188	0.01212639	regulator of chromatin condensation-1 (RCC1)
GmaAffx.91519.1.S1_s_at	CF807244	0.013412317	double-stranded DNA-binding family protein
GmaAffx.29692.1.S1_at	AW348396	0.016772715	chitinase (class II)
GmaAffx.71331.1.S1_at	AW597101	0.018428453	galactosyltransferase family protein
Gma.6640.1.S1_at	BQ628278	0.022040082	haem peroxidase
Gma.8022.1.S1_at	BQ628998	0.024040827	epoxide hydrolase
GmaAffx.24201.1.S1_at	BQ740972	0.025685834	Avr9 elicitor response like protein
Gma.9638.1.A1_at	CA936403	0.029056963	ADR6
Signal transduction			
Gma.3893.1.S1_at	U44850.1	0.002298236	Guanine nucleotide-binding protein subunit beta-like protein (ArcA)
Gma.3286.1.S1_at	BQ298747	0.003021268	putative presenilin
GmaAffx.33721.1.S1_at	BI967195	0.003317825	calcium/calmodulin-dependent protein kinase (CDPK)
Gma.17655.1.S1_at	BE057259	0.003317825	protein phosphatase 2A (PP2A)
Gma.10697.2.S1_at	AW424151	0.003591192	BRI1-associated receptor kinase 1
Gma.10649.1.S1_at	BE659256	0.004034485	BRI1-associated receptor kinase 1
Gma.1965.1.S1_x_at	L01432.1	0.00603523	calmodulin (SCaM-3)
GmaAffx.52826.3.S1_at	BF596503	0.00846925	protein phpsphatase 2C (PP2C)
Gma.7517.1.S1_at	BU548272	0.009290923	U box-containing protein kinase
GmaAffx.50980.1.S1_s_at	BE823095	0.010694912	protein phpsphatase 2C (PP2C)
GmaAffx.57055.1.S1_at	AW203411	0.015413718	mitogen-activated protein kinase
Gma.16954.2.A1_at	BE822903	0.017813909	phospholipase C
GmaAffx.85565.1.S1_at	BE611082	0.018428453	calcium-dependent protein kinase 29 (CDPK)
Gma.7177.2.A1_a_at	BI425372	0.018428453	MHK kinase
GmaAffx.35805.2.S1_at	BF324178	0.019563038	MAP3K delta-1 protein kinase-like
Gma.9902.1.A1_at	AW395328	0.019678474	FUSCA 5 MAP kinase kinase (FUS5)
Gma.2314.1.S1_at	AW310385	0.019678474	FUS3-COMPLEMENTING GENE 1
GmaAffx.21787.1.A1_at	AW348555	0.020429855	CLAVATA1 receptor kinase (CLV1)
GmaAffx.69025.1.S1_at	BM271195	0.020753499	RIO kinase

Table 2: Continued.

C-3 dpi			
Probe set ID	Public ID	Avg *P*-value	Gene
Signal transduction			
GmaAffx.62926.1.S1_at	BE804949	0.020828644	G-protein alpha subunit
Gma.11015.1.S1_at	CD398110	0.023684433	leucine-rich repeat transmembrane protein
Gma.3185.2.S1_at	BM890715	0.023684433	leucine-rich repeat transmembrane protein
GmaAffx.15664.1.S1_at	BE607642	0.024040827	LRR receptor-like protein kinase
GmaAffx.77602.1.S1_at	BQ627622	0.025399823	protein phosphatase-2c (PP2C)
Gma.5722.1.S1_at	BU546228	0.029056963	Ste20-related protein kinase
Gma.8364.1.S1_at	BE659226	0.034312943	putative protein kinase (PK12)
Transcription			
Gma.4165.1.S1_at	BI969143	0.005201937	homeodomain-related
Gma.4205.1.S1_at	AF464906.1	0.005679433	repressor protein
GmaAffx.50673.1.S1_at	BF425742	0.005679433	No apical meristem (NAM) protein
GmaAffx.67609.1.S1_at	BG551013	0.007110254	SAR DNA-binding protein-1
Gma.16172.1.S1_at	CD411627	0.009049965	CONSTANS-like B-box zinc finger
GmaAffx.52855.1.S1_at	AW308923	0.010397582	transcription initiation factor IIE (TFIIE)
Gma.3176.1.S1_a_at	BU549115	0.010649919	transcription factor IIA (TFIIA)
Gma.2702.2.S1_at	AI855587	0.010649919	no apical meristem (NAM)
Gma.8298.1.S1_at	CD392694	0.012696314	trithorax 4-nuclear SET-domain containing protein
Gma.4116.2.S1_at	BM177935	0.014076915	transcription initiation factor IIE, beta subunit (TFIiE beta)
GmaAffx.85579.1.S1_at	BQ273352	0.014307059	lipoamide dehydrogenase
GmaAffx.81234.1.A1_at	BE823765	0.014307059	TRF-LIKE 8 (TRFL8)
GmaAffx.66085.1.S1_at	BQ630399	0.015096504	Basic Helix-Loop-Helix (bHLH)
Gma.13174.1.S1_s_at	CD414686	0.016772715	indoleacetic acid-induced protein 1 (IAA13)
GmaAffx.71523.1.S1_at	BU544012	0.01738237	phospatase 2A inhibitor (NAP1-RELATED PROTEIN 1 [NRP1])
GmaAffx.92212.1.A1_s_at	CF807937	0.018428453	MYB transcription factor (MYB92)
Gma.7891.1.S1_at	AW310625	0.020753499	Basic Helix-Loop-Helix (bHLH)
Gma.3632.1.A1_at	BI316950	0.020828644	zinc finger protein
Gma.17664.1.S1_at	AW348917	0.020828644	zinc finger (DHHC type) family protein
Gma.2243.2.S1_s_at	BE807162	0.022028694	transcription initiation factor IIF beta (TFIIF beta)
Gma.1270.1.S1_at	CD405147	0.022830045	LIM domain-containing, zinc-binding protein
Gma.752.1.A1_at	AW432463	0.022830045	Helix-loop-helix DNA-binding
Gma.5274.1.S1_at	BM178426	0.025399823	transcription factor EIL2
Gma.7776.1.A1_at	CD399260	0.025685834	ATBRM/CHR2
GmaAffx.52970.1.S1_at	BU548330	0.027055562	zinc finger (DHHC type) family protein
Gma.7212.1.S1_at	BE658102	0.027055562	Zinc finger, BED-type predicted
GmaAffx.91768.1.S1_s_at	CF807493	0.031457154	WRKY27

Table 2: Continued.

C-3 dpi			
Probe set ID	Public ID	Avg *P*-value	Gene
Transcription			
Gma.14100.1.S1_at	CD408988	0.034312943	zinc finger, RING-type
GmaAffx.11131.1.A1_at	CD395293	0.037684072	CCR4 associated factor 1-related protein
Gma.4281.1.S1_at	AW156348	0.037684072	WRKY

of gene expression. However, it is possible that very large differences in gene activity are present when the analysis involves comparing gene expression within homogeneous populations of cells, especially cells that are at different stages of differentiation or become genomically reprogrammed as a consequence of a pathological infection. In the analysis presented here, the DCM was used as an alternative method to identify genes that are expressed in a particular cell type but not active in another cell type. Importantly, the resulting DCM analysis identified a group of genes that were present uniquely within a sample type. However, those same genes were eliminated by differential expression analyses methods because differential expression analyses require expression data from each sample in the comparison.

The DCM is a statistically sound method based on a four-step procedure. The procedude incorporates (1) removal of saturated probes, (2) calculation of discrimination scores, (3) *P*-value calculation using the Wilcoxon's rank test, and (4) making the detection call. The DCM has been used in a variety of analyses to understand gene expression in various experimental systems [4–6]. The DCM analyses have demonstrated the utility of the method. The DCM takes into consideration only the presence of the transcript as measured by the probe set on the microarray. Thus, DCM can be used as a measurement of the diversity of transcripts within those samples. In the analysis presented here, DCM identified thousands of genes in the 3 dpi incompatible and compatible syncytium samples, the 8 dpi compatible syncytium samples, and the pericycle samples that were isolated by LCM. The DCM, along with customized computer scripts, was then used to compare the transcripts present in those samples. The method allowed for the identification and comparison of transcripts that were found in those samples. The DCM analyses presented here identified transcripts that are found in the incompatible or compatible syncytium samples that did not meet the criteria in a differential expression analysis [26]. Thus, DCM provided a broader (or different) estimate of the similarities and differences in those samples. In all of the comparisons made, the samples exhibited substantial differences in transcript composition. The DCM demonstrated vast differences in transcripts when directly comparing 3 dpi incompatible to compatible syncytia, even though the anatomy of these cells at that time appears similar [26–28, 33].

Comparisons of detection calls between the pericycle control and syncytia undergoing an incompatible reaction resulted in the identification of a disproportionate number of transcripts in the syncytia undergoing an incompatible reaction belonging to the "No Homology to Known Proteins" category. Conversely, the pericycle control had a disproportionate number of transcripts in the "Metabolism" and "Hypothetical Protein Supported by cDNA" categories (Figure 8(b)). Detection calls can also be used to determine other features of the cells under study. For example, detection calls can be used to arrive at an estimate of how different (or similar) two cell samples or sample types are from each other. Thus, when examining the development of specialized cell types like the syncytium, certain types of gene activity can be identified and used for comparative purposes by using DCM. For example, rapid elicitation of gene expression can be followed by a return to preinfestation levels during a reaction to a pathogen [62, 63]. The DCM may allow for the identification of genes expressed at lower levels that are not identified in a differential expression analysis. The DCM will also identify gene expression that is at a high threshold in one sample and absent in the other. This category of genes would be excluded in a differential expression analysis because no statistics can be performed on probe sets lacking expression data.

In this study, DCM aided in identifying additional genes expressed during nematode infection. In the analyses many genes from (1) Disease and Defense, (2) Signaling, and (3) Transcription categories that were unique to one sample type and thus excluded from a differential expression analysis were focused on because of their obvious importance in a variety of plant defense pathways. The analyses here focus on the incompatible analyses. Recent proteomic work by Afzal et al. [64] provides an additional bank of genes to obtain a broader understanding of *H. glycines* infection of *G. max*. The genes identified in the analysis make reasonable candidates for further functional tests [32].

4.1. DCM Is Used to Compare the 3 dpi Incompatible Syncytium to Pericycle Cells. The DCM analyses identified genes that were present only in the incompatible syncytial cell sample as compared to the pericycle sample. The genes included various defense response genes. Some of these were DRRG49-C (CF809336), Pto-interacting-kinase (Pti) (BI970555), BOTRYTIS-INDUCED KINASE 1 (BIK1) (AW311265), and two leucine-rich repeat genes (LRRs) (AW348555, AW317282). LRRs near *rhg1* exist [65]. The DRRG49-C gene is induced during pathogen attack [66]. The Pti-kinase [67] and BIK1 [68] are examples of genes that are induced during a response to pathogenic attack and are

Table 3: Select genes that were unique to the 8 dpi syncytia undergoing a compatible reaction but that were not differentially expressed as compared to a pericycle control sample (Figure 8(f)) comprising the Disease and Defense, Signaling, and Transcription categories.

C-8 dpi			
Probe set ID	Public ID	Avg *P*-value	Gene
Disease & defense			
GmaAffx.91273.1.S1_s_at	CF805964	0.002747901	wound-induced protein
Gma.4305.1.S1_at	AW350687	0.00337326	haem peroxidase
GmaAffx.90134.1.S1_s_at	CF805859	0.004659843	purple acid phosphatase-like protein
Gma.8512.1.S1_at	AF236108.1	0.014307059	purple acid phosphatase-like protein
Gma.7301.1.S1_at	BM528250	0.019563038	gamma-glutamyl transferase
GmaAffx.78614.1.S1_at	BQ611991	0.019678474	Suppressor-of-White-APricot splicing regulator
GmaAffx.59573.1.S1_at	AW350986	0.019951841	purple acid phosphatase-like protein
GmaAffx.91519.1.S1_s_at	CF807244	0.027055562	double-stranded DNA-binding protein
Gma.11154.1.S1_a_at	AW309927	0.031457154	putative elicitor-responsive gene-3
GmaAffx.83232.1.S1_at	BE023128	0.037684072	MILDEW RESISTANCE LOCUS O 10 (MLO10)
Signal transduction			
Gma.1965.1.S1_x_at	L01432.1	0.001946244	calmodulin (SCaM-3)
GmaAffx.90377.1.S1_s_at	CF806102	0.001946244	PP2A regulatory subunit
Gma.9902.1.A1_at	AW395328	0.002571602	FUSCA 5 MAP kinase kinase (FUS5)
Gma.7517.1.S1_at	BU548272	0.002923594	U box-containing protein kinase
Gma.17655.1.S1_at	BE057259	0.00492857	calcium/calmodulin-dependent protein kinase
GmaAffx.50980.1.S1_at	BE823095	0.007394226	protein phpsphatase 2C (PP2C)
Gma.4455.3.S1_at	CB063632	0.009290923	PROTEIN KINASE 2B (APK2B)
Gma.5188.1.S1_at	AW349454	0.010397582	protein phosphatase type-2C
Gma.9853.1.A1_at	AW350335	0.010397582	LysM domain-containing receptor-like kinase 7
Gma.10515.1.S1_at	BM528701	0.011324733	calmodulin-binding receptor-like cytoplasmic kinase 3 (CRCK3)
Gma.5304.2.S1_at	CD410657	0.01212639	membrane-associated progesterone-binding protein 2 (ATMAPR2)
Gma.1068.1.S1_at	L19360.1	0.013412317	protein kinase 2
Gma.4631.1.S1_at	BE824210	0.013412974	MITOGEN-ACTIVATED PROTEIN KINASE 1 (ATMPK1)
Gma.5722.1.S1_at	BU546228	0.013451556	Ste20-related protein kinase
Gma.596.1.S1_at	AF228501.1	0.015413718	14-3-3-like protein
Gma.2222.1.S1_at	CD416168	0.015413718	Inositol monophosphatase
GmaAffx.82748.1.S1_s_at	BM085604	0.016427052	protein phosphatase 2C (PP2C)
GmaAffx.67957.1.S1_at	BG157622	0.016772715	RhoGAP small G protein family protein
Gma.15250.1.S1_x_at	AI856228	0.016772715	calmodulin
Gma.10649.1.S1_at	BE659256	0.016932704	BRI1-associated receptor kinase 1

Table 3: Continued.

C-8 dpi			
Probe set ID	Public ID	Avg *P*-value	Gene
Signal transduction			
Gma.8364.1.S1_at	BE659226	0.016932704	ARABIDOPSIS FUS3-COMPLEMENTING GENE (AFC1)
Gma.10697.2.S1_at	AW424151	0.01738237	protein phosphatase 2A (PP2A) catalytic subunit
Gma.9706.1.S1_at	BE657400	0.018668953	protein phosphatase 1 (PP1)
GmaAffx.65281.1.S1_at	CA819808	0.019563038	transmembrane protein
Gma.2314.1.S1_at	AW310385	0.022040082	ARABIDOPSIS FUS3-COMPLEMENTING GENE (AFC2)
Gma.10927.1.S1_at	CD398961	0.023684433	root hair defective 3 (RHD3)
Gma.2471.1.S1_at	AI938029	0.025399823	FUSCA PROTEIN (FUS6)
Gma.4629.1.A1_at	CA820195	0.028086024	SGT1
GmaAffx.78968.2.S1_at	BM188587	0.030941813	cysteine protease
Gma.1518.2.S1_a_at	BM524684	0.030941813	cysteine protease
GmaAffx.19821.1.S1_at	CA782536	0.030941813	protein kinase
Gma.4536.1.A1_at	BI945486	0.034312943	receptor-like protein kinase
Transcription			
GmaAffx.92861.1.S1_s_at	CF808586	0.002923594	HMG-protein
Gma.1748.2.S1_a_at	CA820372	0.003591192	no apical meristem (NAM) protein (NAC1)
Gma.17736.1.S1_at	AW598570	0.00603523	zinc finger, C2H2-type
Gma.4165.1.S1_at	BI969143	0.007394226	Homeodomain-related
Gma.6739.1.S1_s_at	AI856042	0.007667593	RNA polymerase II (RPB15.9)
Gma.2844.1.S1_at	BI972378	0.008019584	auxin-induced protein 2
Gma.2258.2.S1_a_at	BG237280	0.008396837	pre-mRNA processing ribonucleoprotein (NOP5)
GmaAffx.54382.1.A1_at	BE807592	0.00846925	calmodulin-binding transcription activator 4
GmaAffx.50673.1.S1_at	BF425742	0.009049965	no apical meristem (NAM) protein
GmaAffx.41946.1.S1_at	BM528357	0.009290923	helix-loop-helix DNA-binding
GmaAffx.78992.1.S1_at	BU760819	0.010397582	HMG-I and HMG-Y DNA-binding protein
Gma.2465.1.S1_at	CD390577	0.010694912	ARABIDOPSIS THALIANA HOMEOBOX PROTEIN 54 (ATHB54)
GmaAffx.42667.1.S1_at	BU761164	0.011051366	SCARECROW-LIKE 1 (SCL1)
GmaAffx.66085.1.S1_at	BQ630399	0.011411572	basic helix-loop-helix (bHLH)
Gma.4975.1.S1_at	BI970178	0.011756578	zinc finger, CCCH-type; Zinc finger, RING-type
Gma.6838.1.S1_at	AW349633	0.011756578	NIM1-like protein 1 (NPR-1)
GmaAffx.91768.1.S1_s_at	CF807493	0.013412317	WRKY27
GmaAffx.81622.1.S1_at	BM093159	0.013412317	bZIP transcription factor bZIP123
Gma.3609.1.S1_at	CD392010	0.013412317	helix-loop-helix DNA-binding
GmaAffx.85579.1.S1_at	BQ273352	0.014307059	lipoamide dehydrogenase-UNE12 (unfertilized embryo sac 12)
GmaAffx.60479.4.S1_at	BG507369	0.014307059	BEL1-like homeodomain transcription factor

Table 3: Continued.

C-8 dpi			
Probe set ID	Public ID	Avg *P*-value	Gene
Transcription			
GmaAffx.24357.1.A1_at	BU544827	0.014526581	zinc finger (DHHC type) family protein
Gma.7212.1.S1_at	BE658102	0.016772715	SUPPRESSOR OF FRIGIDA4 (SUF4)
Gma.3632.1.A1_at	BI316950	0.016772715	zinc finger protein
Gma.15748.1.A1_at	AI900530	0.017813909	WRKY15
Gma.16645.1.S1_at	BM143429	0.017952293	no apical meristem (NAM) protein (NAC2)
Gma.4225.1.S1_a_at	AW317387	0.018428453	transcription initiation factor IID (TFIID)
Gma.1772.1.S1_at	CD406036	0.019678474	transcription factor IIA (TFIIA)
Gma.16172.1.S1_at	CD411627	0.020429855	CONSTANS-like B-box zinc finger
GmaAffx.65829.1.A1_at	CD392418	0.020669698	pathogenesis-related transcriptional factor and ERF
Gma.4281.1.S1_at	AW156348	0.020669698	WRKY
Gma.12798.1.S1_at	CD390501	0.020828644	PHYTOCHROME A SIGNAL TRANSDUCTION 1 (PAT1)
GmaAffx.85720.1.S1_at	CD415193	0.022040082	basic helix-loop-helix (bHLH)
GmaAffx.87860.1.S1_at	BU081275	0.023684433	MYB transcription factor
Gma.11345.1.S1_at	BE024036	0.025230236	MYB transcription factor (MYB92)
GmaAffx.41422.2.S1_at	BI321807	0.027055562	PHD1
GmaAffx.552.1.S1_at	BI785020	0.027055562	RNA polymerase dimerisation domain containing protein (Rpb3/Rpb11)
GmaAffx.37827.1.S1_at	CD414912	0.028086024	gibberellic acid-insensitive mutant protein 1 (GAI1)/DELLA protein
GmaAffx.73813.1.S1_at	BU551266	0.029056963	Arabidopsis NAC domain containing protein 104 (ANAC104/XND1)
GmaAffx.67609.1.S1_at	BG551013	0.029056963	SAR DNA-binding protein-1
GmaAffx.91229.1.S1_s_at	CF806954	0.030941813	AUXIN RESISTANT 3 (AXR3)
GmaAffx.1957.1.S1_at	BM271285	0.030941813	WIP1 protein
Gma.4207.3.S1_a_at	BE804803	0.031457154	MYB transcription factor (MYB48)

involved in important defense responses. The identification of a Pti-like kinase was particularly interesting. In *L. esculentum*, *Pti4* and *Pti5* are induced by the virulent *Pseudomonas syringae* pv. *tomato*, the nonhost pathogenic bacterium *Xanthomonas oryzae* pv. *oryzae* (strain PXO^{A} *avrXa10*), and the nonpathogenic bacterium *Pseudomonas fluorescens* (strain 2–79) [69]. Interestingly, Pti kinases are observed at 3 dpi in both compatible and incompatible reactions. The Pti-kinase identified in the 3 dpi incompatible reaction was most closely related to *Pti1* isolated from tomato [70]. In that analysis, *Pti1* was shown to be phosphorylated by *Pto* and to be involved in the hypersensitive response [70]. The LRR genes have a long history as being important for plant defense [71, 72]. The genes also have been shown to confer resistance to parasitic nematodes [73–78]. Thus, due to the transient nature of expression of some of these genes in other systems, it is not surprising that they were not identified as being differentially expressed in syncytium samples [26].

4.2. DCM Is Used to Compare the 3 dpi Incompatible Syncytium Directly to the 3 dpi Compatible Syncytium. The DCM analyses identified genes that were present only in the 3 dpi incompatible syncytium as compared directly to the 3 dpi compatible syncytium sample (supplementary Table 12). The probe sets included genes like

Table 4: An analysis compared the 3 dpi syncytia undergoing an incompatible reaction directly to the 3 dpi compatible syncytium samples. Selected genes that were unique to the 3 dpi syncytia undergoing an incompatible reaction but that were not differentially expressed as compared directly to the 3 dpi compatible syncytium samples (Figure 8(h)) comprising the Disease and Defense, Signaling, and Transcription categories are provided.

I-3 dpi genes in the comparison of I-3 dpi to C-3 dpi			
Probe set ID	Public ID	Avg *P*-value	Gene
Disease & defense			
Gma.4886.2.S1_at	AW234624	0.005201937	haem peroxidase
Gma.405.1.A1_at	AI443411	0.008396837	leucine-rich repeat family protein (DRT100)
Gma.2044.2.S1_at	BE821230	0.011411572	abscisic stress ripening-like protein
GmaAffx.92230.1.A1_s_at	CF807955	0.012305657	thaumatin-like protein PR-5b
Gma.7542.2.S1_at	CA936764	0.016772715	defender against cell death 1 (DAD-1)
Gma.8449.1.S1_s_at	AF002258.1	0.019563038	CoA ligase 4
GmaAffx.14986.1.S1_at	BE657889	0.020669698	PHOSPHATE-INDUCED 1 (phi-1)
GmaAffx.2203.1.S1_at	CD415745	0.020669698	cadmium-induced protein
GmaAffx.91141.1.S1_at	CF806866	0.020828644	peroxidase 1 precursor
GmaAffx.46214.1.S1_at	BE659266	0.022934167	polyphenol oxidase
Signal transduction			
Gma.13604.1.S1_at	CD401537	0.011411572	protein kinase
GmaAffx.56323.1.S1_at	BU764214	0.01212639	protein kinase
Gma.6092.1.S1_at	BI968757	0.012305657	COP9 signalosome subunit 3
Gma.5162.1.A1_at	BI971156	0.013412317	Curculin-like (mannose-binding) lectin protein kinase
Gma.4455.3.S1_at	CB063632	0.014076915	PROTEIN KINASE 2B (APK2B)
GmaAffx.66511.1.S1_at	AW350917	0.019563038	calcium and calmodulin-dependent protein kinase (ATCDPK1)
GmaAffx.34312.1.S1_at	AI965735	0.023684433	protein phosphatase 2C (PP2C)
GmaAffx.64402.1.S1_at	AW317282	0.025399823	leucine-rich repeat
Gma.4801.1.S1_s_at	BU548608	0.028086024	protein phosphatase 1 (PP1)
Gma.11291.1.S1_at	AW351207	0.028086024	inositol 1,3,4-trisphosphate 5/6-kinase
GmaAffx.73451.1.S1_at	BG046889	0.034312943	CALMODULIN-RELATED PROTEIN 2
Transcription			
GmaAffx.89077.1.A1_s_at	CK605647	0.009323331	CONSTANS interacting protein 2a
Gma.3996.1.S1_at	AW394946	0.014307059	WRKY52
Gma.9678.1.S1_at	CD404894	0.016707249	RNA polymerase II
Gma.12330.2.S1_s_at	BI972758	0.027055562	pathogenesis-related transcriptional factor
Gma.6838.1.S1_at	AW349633	0.027055562	NIM1-like protein 1 (NPR-1)
Gma.16645.1.S1_at	BM143429	0.028086024	Arabidopsis NAC domain-containing protein 1 (ATAF1)

Table 5: An analysis compared the 3 dpi syncytia undergoing an incompatible reaction directly to the 3 dpi compatible syncytium samples. Selected genes that were unique to the 3 dpi syncytia undergoing a compatible reaction but that were not differentially expressed as compared directly to the 3 dpi incompatible syncytium samples (Figure 8(h)) comprising the Disease and Defense, Signaling, and Transcription categories.

C-3 dpi genes in the comparison of I-3 dpi to C-3 dpi			
Probe set ID	Public ID	Avg *P*-value	Gene
Disease & defense			
GmaAffx.36484.1.S1_s_at	BI425441	0.001672877	PR1a
Gma.6091.1.S1_at	AW310762	0.00221961	haem peroxidase
Gma.2523.1.S1_s_at	CA852440	0.002747901	R 14 protein
GmaAffx.85114.1.S1_s_at	AW760844	0.003021268	Malus major allergen (Mal d 1.07)
Gma.4312.3.S1_a_at	BF424240	0.003822926	glutathione peroxidase (GSH-PX3)
Gma.257.2.S1_a_at	CD400364	0.005553929	cysteine proteinase inhibitor
GmaAffx.36514.1.S1_at	BE658341	0.005553929	cationic peroxidase
Gma.6299.3.S1_at	BU547701	0.00603523	selenium binding protein
GmaAffx.92699.1.S1_s_at	CF808424	0.006308596	PR-5 protein
Gma.5141.1.S1_at	BI971102	0.007667593	laccase 3 (LAC3)
Gma.9504.1.S1_at	CA803130	0.007680178	plant disease resistance response protein
Gma.18084.1.S1_at	BI317557	0.008396837	RESPIRATORY BURST OXIDASE HOMOLOG (ATRBOHB)
Gma.8144.1.A1_at	BU548599	0.009323331	cationic peroxidase
GmaAffx.11893.1.A1_at	CD414188	0.01212639	regulator of chromatin condensation-1 (RCC1)
Gma.4077.1.S1_at	CD414118	0.012696314	ASR protein
Gma.7257.2.S1_at	BG155489	0.016427052	soluble epoxide hydrolase
GmaAffx.71331.1.S1_at	AW597101	0.018428453	galactosyltransferase family protein
GmaAffx.52146.1.S1_at	CA934966	0.028086024	PATHOGENESIS-RELATED 4 (PR4)
Gma.9638.1.A1_at	CA936403	0.029056963	ADR6
Signal transduction			
GmaAffx.92136.1.S1_s_at	CF807451	0.001672877	Curculin-like (mannose-binding) lectin protein kinase
Gma.6338.1.S1_at	AI442775	0.001946244	protein phosphatase 2C (PP2C)
Gma.3893.1.S1_at	U44850.1	0.002298236	Arabidopsis thaliana Homolog of the Tobacco ArcA (ATARCA)
Gma.4228.1.S1_at	AI856764	0.002298236	RelA-SpoT like protein (RSH3)
Gma.13033.1.A1_a_at	CD392795	0.002298236	calcium-dependent calmodulin-independent protein kinase (CDPK)
Gma.6709.1.S1_at	BE823291	0.002747901	CBL-interacting protein kinase 22
Gma.10697.2.S1_at	AW424151	0.003591192	protein phosphatase 2A catalytic subunit
Gma.11006.1.S1_s_at	AW706204	0.00492857	CBL-interacting protein kinase
Gma.6359.1.S1_at	CD398481	0.005201937	caltractin-like
GmaAffx.92229.1.S1_s_at	CF806381	0.005553929	14-3-3 protein
Gma.4507.1.S1_at	BG653255	0.006308596	leucine-rich repeat protein
Gma.568.1.S1_at	BI967984	0.007110254	LRR receptor-like protein kinase

Table 5: Continued.

C-3 dpi genes in the comparison of I-3 dpi to C-3 dpi			
Probe set ID	Public ID	Avg *P*-value	Gene
Signal transduction			
GmaAffx.90655.1.S1_s_at	CF806380	0.007680178	14-3-3-like protein C (SGF14C)
GmaAffx.91570.1.A1_s_at	CF807732	0.008019584	JUN-activation-domain-binding protein
Gma.4049.1.S1_at	BQ786519	0.008184263	wall-associated kinase (WAK-like kinase)
Gma.3083.1.S1_at	BE474466	0.008396837	BAK1 (BRI1-ASSOCIATED RECEPTOR KINASE)
Gma.7517.1.S1_at	BU548272	0.009290923	protein kinase
GmaAffx.25928.1.S1_at	CD414013	0.012305657	WD-40 repeat protein
Gma.15907.1.A1_at	CD407154	0.014307059	leucine-rich repeat protein
Gma.3852.1.S1_at	CD399104	0.014771313	serine/threonine-protein phosphatase PP1
GmaAffx.57055.1.S1_at	AW203411	0.015413718	Arabidopsis thaliana MAP kinase 2 (ATMPK20)
Gma.10215.1.S1_a_at	AY263347.1	0.016307345	Pti1-like kinase
GmaAffx.85565.1.S1_at	BE611082	0.018428453	calcium-dependent protein kinase 29 (CPK29)
Gma.7177.2.A1_a_at	BI425372	0.018428453	Cdc2-related protein kinase (CRK2)
GmaAffx.35805.2.S1_at	BF324178	0.019563038	MAP3K delta-1 protein kinase-like
Gma.10798.1.S1_at	CD401168	0.019563038	protein phosphatase 2A (PP2A)
Gma.2314.1.S1_at	AW310385	0.019678474	ARABIDOPSIS FUS3-COMPLEMENTING GENE (AFC2)
Gma.1517.2.S1_a_at	BE059859	0.019951841	calcium dependent calmodulin independent protein kinase (CDPK)
Gma.6123.1.S1_at	AW349800	0.020669698	VERNALIZATION INDEPENDENCE 3 (VIP3)
GmaAffx.69025.1.S1_at	BM271195	0.020753499	RIO kinase
GmaAffx.62926.1.S1_at	BE804949	0.020828644	extra-large GTP-binding protein 3 (XLG3)
GmaAffx.40750.1.S1_s_at	BG352469	0.022028694	protein phosphatase 2A regulatory subunit (PP2A)
GmaAffx.44305.1.S1_at	BU551393	0.022830045	transmembrane protein
Gma.3185.2.S1_at	BM890715	0.023684433	leucine-rich repeat transmembrane protein
Gma.11015.1.S1_at	CD398110	0.023684433	leucine-rich repeat transmembrane protein
GmaAffx.15664.1.S1_at	BE607642	0.024040827	leucine-rich repeat transmembrane protein
Gma.1423.1.S1_s_at	AI960045	0.024040827	BRASSINAZOLE-RESISTANT 1 (BZR1)
Gma.4044.1.S1_at	BE821233	0.025399823	Pescadillo-like
GmaAffx.89525.1.S1_s_at	CK606517	0.027055562	protein phosphatase 1 (PP1)
Gma.7387.1.A1_a_at	CD396910	0.027055562	pseudo-response regulator
Gma.5722.1.S1_at	BU546228	0.029056963	Ste20-related protein kinase

Table 5: Continued.

C-3 dpi genes in the comparison of I-3 dpi to C-3 dpi			
Probe set ID	Public ID	Avg *P*-value	Gene
Transcription			
Gma.1538.1.S1_a_at	AW351115	0.002298236	salt tolerance protein 6
Gma.12279.1.A1_at	CD397826	0.00337326	basic helix-loop-helix (bHLH)
Gma.5331.1.S1_at	BI892702	0.004307852	no apical meristem (NAM) protein NAC4
Gma.593.2.S1_x_at	CA800286	0.00492857	MYB transcription factor (MYB173)
GmaAffx.5069.2.A1_at	BM121565	0.005201937	basic-leucine zipper (bZIP111)
GmaAffx.50673.1.S1_at	BF425742	0.005679433	no apical meristem (NAM) protein (NAC)
GmaAffx.93436.1.A1_s_at	CF809161	0.007680178	AP2/EREBP transcription factor ERF-2
GmaAffx.38951.1.S1_at	BI322098	0.008396837	basic-leucine zipper (bZIP)
Gma.16172.1.S1_at	CD411627	0.009049965	CONSTANS-LIKE 13
Gma.3730.2.S1_a_at	BI320846	0.009290923	WRKY27
Gma.15862.1.S1_at	BI970593	0.009323331	pathogenesis-related transcriptional factor and ERF
Gma.2702.2.S1_at	AI855587	0.010649919	no apical meristem (NAM) protein
Gma.163.1.S1_at	AB029269.1	0.014076915	MYB transcription factor (MYB12)
Gma.16613.1.S1_s_at	BU760651	0.014307059	zinc finger
GmaAffx.81234.1.A1_at	BE823765	0.014307059	MYB-TRFL8 (TRF-LIKE 8)
GmaAffx.15471.1.S1_at	BQ611747	0.014526581	MYB transcription factor (MYB139)
Gma.17432.1.S1_s_at	AW277783	0.015813164	RNA polymerase subunit (RPB5)
Gma.13174.1.S1_s_at	CD414686	0.016772715	aux/IAA protein (IAA13)
GmaAffx.71523.1.S1_at	BU544012	0.01738237	Polycomb group-NAP1-RELATED PROTEIN 1 (NRP1)
Gma.15460.1.S1_at	CD403496	0.018032044	ethylene-induced calmodulin binding protein (EICBP.B)
GmaAffx.92212.1.A1_s_at	CF807937	0.018428453	MYB transcription factor (MYB92)
Gma.5483.1.S1_s_at	CD414581	0.019563038	basic-leucine zipper (bZIP105)
Gma.7891.1.S1_at	AW310625	0.020753499	basic helix-loop-helix
Gma.3632.1.A1_at	BI316950	0.020828644	zinc finger protein
Gma.17664.1.S1_at	AW348917	0.020828644	zinc finger (DHHC type) family protein
Gma.752.1.A1_at	AW432463	0.022830045	helix-loop-helix DNA-binding
Gma.7341.1.A1_s_at	CA953350	0.022830045	aux/IAA protein (IAA3)
GmaAffx.44143.1.S1_at	BU547730	0.023684433	CCR4-Not complex component (Not1)
GmaAffx.50295.1.S1_at	BI424123	0.024040827	zinc finger (C2H2 type, AN1-like)
GmaAffx.76537.1.S1_at	CD416417	0.025399823	MYC1
Gma.5274.1.S1_at	BM178426	0.025399823	transcription factor EIL2
GmaAffx.91768.1.S1_s_at	CF807493	0.031457154	WRKY27
Gma.6571.2.S1_a_at	BE191621	0.031457154	transcription initiation factor IIA (TFIIA)
Gma.4281.1.S1_at	AW156348	0.037684072	WRKY

Table 5: Continued.

C-3 dpi genes in the comparison of I-3 dpi to C-3 dpi			
Probe set ID	Public ID	Avg *P*-value	Gene
Transcription			
Gma.15184.1.S1_at	BM522992	0.037684072	homeobox-leucine zipper protein 22 (HAT22)

haem peroxidase (AW234624), DRT100 (AI443411), thaumatin (CF807955), defender against cell death-1 (DAD-1) (CA936764), polyphenol oxidase (BE659266), calcium dependent protein kinase (AW350917), constitutive photomorphogenic 9 (COP9) subunit 3 (BI968757), WRKY 52 gene (AW394946), and Nonexpressor of PR genes 1 (NPR1) (AW349633) in syncytia undergoing an incompatible reaction at 3 dpi. Importantly, these comparisons were made directly to syncytia undergoing a compatible reaction at 3 dpi. Haem peroxidase [79], DRT100 [80, 81], thaumatin [82], DAD-1 [83–85], polyphenol oxidase [86–88], calcium dependent protein kinase [89, 90], COP9 subunit 3 [91, 92], WRKY [93–99], and NPR1 [100] all perform important roles in defense and/or stress tolerance. Genes like polyphenol oxidase are known to exhibit intense, but transient expression after wounding [87] while a WRKY homolog (WRKY45) exhibits intense, but transient expression after infection [99]. The identification of genes that are known to experience rapid elicitation of gene expression as a consequence of wounding or infection followed by a rapid decline in expression is consistent with their absence from differential expression analyses. The absence could be due to the chronology of infection and syncytium establishment and maintenance [27–29, 36, 57–61].

4.3. DCM Identifies Genes Involved in Defense in the Syncytia Undergoing an Incompatible Reaction. Comparisons of 3 dpi resistant syncytia to 3 dpi susceptible syncytia resulted in the identification of polyphenol oxidase (PPO). PPO, also known as catechol oxidase, is an important protein in the defense response, being responsible for catalyzing the oxidation of *o*-diphenols to *o*-diquinones, thereby having diphenolase activity. In some plants, PPO may also perform the *o*-hydroxylation of monophenols, thereby having monophenolase activity [101]. Cellular components react rapidly to the *o*-quinones, whereby they rapidly polymerize and alkylate cell components. Consequently, tissue becomes brown in coloration because of extensive cross-linking of phenols, proteins, and other cellular constituents [102–106]. Such morphological changes are observed in *G. max* roots undergoing infection by *H. glycines*. Functional tests of PPO activity on pathogens were made in (*Populus tremula* × *P. alba*) plants overexpressing a hybrid poplar (*Populus trichocarpa* × *P. deltoides*) PPO (PtdPPO1) gene [88]. Functional tests demonstrate that PPO-overexpressing transgenic plants produce significantly higher mortality and reduced average weight gain in the forest tent caterpillar (*Malacosoma disstria*) larvae feeding on transgenic plants as compared to control plants [88]. Similar experiments, involving the overexpression of a potato (*Solanum tuberosum* L.) PPO in tomato (*Lycopersicon esculentum* Mill. cv. Money Maker), resulted in transgenic plants expressing 30-fold more PPO transcripts [107]. Quantification of PPO protein functionality showed a 5- to 10-fold increase in PPO activity in the transgenic plants [107]. Consequently, the overexpressing PPO transgenic lines produce 15-fold fewer lesions as well as strong inhibition of bacterial growth [107]. Bacterial population growth counts demonstrate at least a 100-fold reduction of bacterial populations in the infected leaves [107]. Thus, PPO could provide a terminal step in plant defense and may provide a localized resistance reaction to *H. glycines* infection.

WRKY transcription factor homologs, involved directly in plant defense, are also identified in syncytia undergoing a resistant reaction. WRKY transcription factors are important in defense [93–96, 98, 108]. Shen et al. [108] demonstrated that WRKY genes are important to the resistance response in the specific cells that contain the signaling proteins that are secreted by the pathogen. Shen et al. [108] demonstrated that this is accomplished through leucine rich repeat receptor-like kinase genes (LRRs) involved in resistance. Many LRRs are essential in gene-for-gene resistant (R) interactions [72]. Shen et al. [108] demonstrated that the signals were transduced through R-genes to WRKY transcription factors, resulting in resistance to the pathogen. Importantly, R genes have been shown to confer resistance to parasitic nematodes [73, 75]. WRKY gene expression in the syncytial cells during the resistance response is consistent with their suggested roles in plant defense.

The nonexpressor of PR genes (NPR1) (also known as *nim1* (for noninducible immunity 1) and *sai1*) [109, 110] is the regulator of salicylic acid-mediated defense. Mutants of NPR1 block SA signaling in *A. thaliana* [100, 110–112]. In the uninduced state, NPR1 exists in the cytoplasm as an oligomer. The oligomer is formed through intermolecular disulfide bonds [113]. Oligomerization is mediated by S-nitrosylation of NPR1 by S-nitrosoglutathione which occurs at cysteine-156 [114]. During systemic acquired resistance (SAR), NPR1 experiences a thioredoxin-mediated reaction that results in its monomerization [114]. This monomerization is induced by mutations at residues Cys82 and Cys216 that facilitated NPR1 monomer accumulation. It also resulted in constitutive nuclear localization. Importantly, the monomerization promoted NPR1-mediated gene expression in the absence of the pathogen [114]. Experiments in *A. thaliana* using mutants in NPR1 (*npr1-2* and *npr1-3*), impaired in SA signaling, demonstrate an increased susceptibility to the beet cyst nematode *H. schachtii*

Table 6: Select genes that were unique to the 8 dpi syncytia undergoing a compatible reaction but that were not differentially expressed as compared directly to the 3 dpi compatible syncytium samples (Figure 8(j)) comprising the Disease and Defense, Signaling, and Transcription categories.

C-8 dpi as compared to C-3 dpi			
Probe set ID	Public ID	Avg *P*-value	Gene
Disease & defense			
GmaAffx.8704.2.S1_at	BG042982	0.003021268	Peroxidase
Gma.8512.1.S1_at	AF236108.1	0.014307059	purple acid phosphatase
GmaAffx.93342.1.S1_s_at	CF809067	0.014526581	glutathione peroxidase 1
Gma.7301.1.S1_at	BM528250	0.019563038	GAMMA-GLUTAMYL TRANSPEPTIDASE 3 (GGT3)
GmaAffx.59573.1.S1_at	AW350986	0.019951841	purple acid phosphatase
Gma.13182.1.S1_at	CD392298	0.020669698	copper-binding protein (CUTA)
Gma.320.1.S1_at	AF019116.1	0.024040827	Peroxidase
Gma.11154.1.S1_a_at	AW309927	0.031457154	elicitor-responsive gene
Signal transduction			
GmaAffx.21217.3.S1_at	AW569872	0.004392849	protein phosphatase 2C (PP2C)
Gma.4455.3.S1_at	CB063632	0.009290923	PROTEIN KINASE 2B (APK2B)
Gma.2407.1.S1_at	BI970419	0.009755834	putative protein kinase
Gma.5304.2.S1_at	CD410657	0.01212639	membrane-associated progesterone-binding protein 2 (ATMAPR2)
Gma.1007.1.S1_a_at	CD402215	0.015096504	calmodulin-related protein
Gma.2222.1.S1_at	CD416168	0.015413718	inositol monophosphatase
Gma.596.1.S1_at	AF228501.1	0.015413718	14-3-3-like protein
GmaAffx.67957.1.S1_at	BG157622	0.016772715	RhoGAP small G protein family protein
GmaAffx.73932.1.S1_s_at	BU550426	0.017952293	CTR1-like protein kinase
Gma.4487.2.S1_at	AW508329	0.020753499	calcium ion binding
GmaAffx.91867.1.S1_x_at	CF807592	0.028086024	14-3-3 protein
Gma.4629.1.A1_at	CA820195	0.028086024	SGT1
Gma.1518.2.S1_a_at	BM524684	0.030941813	cysteine protease
GmaAffx.19821.1.S1_at	CA782536	0.030941813	serine/threonine protein kinase
Transcription			
GmaAffx.92861.1.S1_s_at	CF808586	0.002923594	HIGH MOBILITY GROUP B 1 (HMGB1)
Gma.3419.2.S1_at	BE658641	0.005201937	zinc finger, C2H2-type
Gma.6739.1.S1_s_at	AI856042	0.007667593	RNA polymerase II 15.9 (RPB15.9)
GmaAffx.41946.1.S1_at	BM528357	0.009290923	helix-loop-helix DNA-binding
GmaAffx.42667.1.S1_at	BU761164	0.011051366	SCARECROW-LIKE 1 (SCL1)
Gma.6476.2.S1_x_at	BQ453135	0.011324733	polynucleotidyl transferase
GmaAffx.30434.1.S1_at	BQ081227	0.011676724	helix-loop-helix DNA-binding
Gma.4975.1.S1_at	BI970178	0.011756578	zinc finger, CCCH-type-RING-type
Gma.6838.1.S1_at	AW349633	0.011756578	NIM1-like protein 1 (NPR-1)
GmaAffx.58899.1.S1_at	BI317760	0.016307345	C2-H2 zinc finger protein
Gma.16645.1.S1_at	BM143429	0.017952293	no apical meristem (NAM) protein (NAC2)
GmaAffx.65829.1.A1_at	CD392418	0.020669698	pathogenesis-related transcriptional factor and ERF

Table 6: Continued.

C-8 dpi as compared to C-3 dpi			
Probe set ID	Public ID	Avg *P*-value	Gene
Transcription			
GmaAffx.53755.1.S1_at	BQ454195	0.022028694	BEL-like homeodomain protein 3
GmaAffx.73306.1.S1_at	BE658301	0.022040082	single-stranded nucleic acid binding R3H
GmaAffx.87860.1.S1_at	BU081275	0.023684433	MYB transcription factor
Gma.11345.1.S1_at	BE024036	0.025230236	MYB transcription factor (MYB92)
GmaAffx.90313.1.S1_s_at	CF806038	0.025685834	no apical meristem (NAM) protein NAC5
GmaAffx.73813.1.S1_at	BU551266	0.029056963	Arabidopsis NAC domain containing protein 104 (ANAC104/XND1)
GmaAffx.1957.1.S1_at	BM271285	0.030941813	WIP1 protein
Gma.8118.1.A1_at	BE819846	0.031457154	zinc finger, C3HC4-type RING finger

[115]. Conversely, the *npr1*-suppressor mutation *sni1* shows decreased susceptibility to the nematode [115]. Thus, the highly induced expression of thioredoxin during the resistance responses of *G. max*$_{[PI\ 548402/Peking]}$ is consistent with functional tests involving *npr1-2* and *npr1-3* in *A. thaliana*. Induced levels of NPR1 are not observed in syncytium samples of *G. max*$_{[PI\ 548402/Peking]}$. Thioredoxin has been shown to be involved in this process [114]. Therefore, it is possible that thioredoxin transcription accompanies infection. Thus, thioredoxin could be recruited during the defense response to monomerize NPR1 already present in root tissues to accomplish the resistant reaction.

Calmodulin dependent protein kinases (CDPKs) such as calmodulin kinase II (CaMKII) are proteins reliant on calcium for their proper function. The identification of CaMKII indicates that calcium may be playing important roles in resistance. Calcium performs many interesting cellular roles. Calcium, as a second messenger, encodes information through Ca^{+2} gradients, amplitude, and oscillation frequency [116]. Thus, proteins relying on Ca^{+2} gradients and calmodulin may be important during the establishment of the resistant reaction. CaMKII functions by decoding Ca^{+2} oscillation frequencies [117]. At the cellular level, calmodulin is implicated in successful plant-pathogen interactions by its interaction with CDPKs. For example, the arbuscular mycorrhizal interaction in *Medicago truncatula* requires the CDPK, DMI3 [118]. Other symbioses as well are dependent on CDPKs [118, 119]. The expression analyses show that calmodulin may be performing some function analogous to those observed for the arbuscular mycorrhizal interaction in *M. truncatula.*

4.4. Orthogonality of the DCM. The DCM has resulted in the identification of probe sets that measure detectable amounts of gene activity in one cell type (present) while absent in the other cell type (Figures 7 and 8). The DCM analysis has also identified genes that were common to the two cell types under investigation. As would be expected, there is orthogonality of the DCM probe set lists as compared to probe set lists obtained by the differential expression analysis method. However, since statistical analyses for differential expression analyses can only happen if statistically significant (e.g., measuring present) amounts of gene activity are present in the two cell types under study (e.g., $\underline{A} \cup \underline{B}$), many genes are eliminated from differential expression analyses. The elimination of the genes occurs because measureable amounts of gene activity as measured by a particular probe set are not present in one of the two samples under study. The exclusion of genes from differential expression analyses is probably less common and less of a problem when the RNA under study is obtained from a whole organism or whole organs (i.e., roots). The problem would be minimized in analyses of whole organisms or organs because they are composed of heterogeneous cell populations, each having unique gene expression programs. The RNA pools of those individual cell types become homogenized during the RNA extraction procedures. In contrast, LCM purifies cells to near homogeneity. Thus, gene expression of homogeneous samples of one cell type may be very different from gene expression found in their neighboring cells or a cell at an earlier point during its developmental process. As shown here, many genes are excluded from a differential expression analysis of nearly homogeneous populations of pericycle cells as compared to syncytia at various stages of their resistant or susceptible reactions. The genes identified in the DCM analyses that are present, but not differentially expressed, became the focus of the analysis presented here. As shown in the multiple analyses, genes that pertain to important classes of genes involved in various plant defense responses to pathogens have been identified by DCM.

5. Summary

The DCM was used to compare syncytium and pericycle samples isolated by LCM. The comparisons presented here are an alternative method of examining microarray gene expression data and are different from those presented in a differential expression analysis of the syncytium [26]. The DCM comparisons are powerful when considering that the cells under investigation are homogeneous (e.g., syncytia). The power of DCM is that it reveals that nearly homogeneous populations of cells have gene activity that is unique to each type. Importantly, differential expression analyses would miss the uniqueness of gene activity of the various cell types because gene expression data is required from each cell type for the analysis to be performed. Therefore, differential expression analyses actually may be underestimating the uniqueness of gene activity profiles for the different cell types under study. The genes identified here represent an additional and significant pool to take into consideration and explore with regard to the interaction between *G. max* and *H. glycines*. The genes can be investigated in functional analyses to study the interaction between *G. max* and *H. glycines* [31, 120]. In the broader sense, DCM should be seriously considered as an analysis tool when comparing homogeneous populations of cells.

Abbreviations

EST: Expressed sequence tag
hpi: Hours post inoculation
dpi: Days post inoculation
J2: Second stage juvenile
FS: Farmer's solution
PFA: Paraformaldehyde
DEPC: Diethylpyrocarbonate
LCM: Laser capture microdissection
MRS: Moisture replacement system
DCM: Detection call methodology.

Acknowledgments

The authors greatly appreciate the continued support provided by the United Soybean Board under Grant 5214. The authors thank Dr. David Munroe and Nicole Lum at the Laboratory of Molecular Technology, SAIC-Frederick, National Cancer Institute at Frederick, Frederick, MD 21701, USA for the Affymetrix array hybridizations and data acquisition. Brandon Le and Anhthu Bui of Dr. Robert Goldberg's lab (University of California-Los Angeles) very kindly provided the *G. max* annotations. The authors thank Veronica Martins for careful editing of the manuscript. Mention of trade names or commercial products in this article is solely for the purpose of providing specific information and does not imply recommendation or endorsement by the United States Department of Agriculture.

References

[1] M. Schena, D. Shalon, R. W. Davis, and P. O. Brown, "Quantitative monitoring of gene expression patterns with a complementary DNA microarray," *Science*, vol. 270, no. 5235, pp. 467–470, 1995.

[2] K. Birnbaum, D. E. Shasha, J. Y. Wang, et al., "A gene expression map of the *Arabidopsis* root," *Science*, vol. 302, no. 5652, pp. 1956–1960, 2003.

[3] A. A. Hill, C. P. Hunter, B. T. Tsung, G. Tucker-Kellogg, and E. L. Brown, "Genomic analysis of gene expression in *C. elegans*," *Science*, vol. 290, no. 5492, pp. 809–812, 2000.

[4] J. Seo, M. Bakay, Y. W. Chen, S. Hilmer, B. Shneiderman, and E. P. Hoffman, "Interactively optimizing signal-to-noise ratios in expression profiling: project-specific algorithm selection and detection p-value weighting in Affymetrix microarrays," *Bioinformatics*, vol. 20, no. 16, pp. 2534–2544, 2004.

[5] J. N. McClintick and H. J. Edenberg, "Effects of filtering by present call on analysis of microarray experiments," *BMC Bioinformatics*, vol. 7, article 49, 2006.

[6] T. Rème, D. Hose, J. De Vos, et al., "A new method for class prediction based on signed-rank algorithms applied to Affymetrix® microarray experiments," *BMC Bioinformatics*, vol. 9, article 16, 2008.

[7] V. Poroyko, L. G. Hejlek, W. G. Spollen, et al., "The maize root transcriptome by serial analysis of gene expression," *Plant Physiology*, vol. 138, no. 3, pp. 1700–1710, 2005.

[8] C. Jung and U. Wyss, "New approaches to control plant parasitic nematodes," *Applied Microbiology and Biotechnology*, vol. 51, no. 4, pp. 439–446, 1999.

[9] G. Gheysen and C. Fenoll, "Gene expression in nematode feeding sites," *Annual Review of Phytopathology*, vol. 40, pp. 191–219, 2002.

[10] V. M. Williamson and A. Kumar, "Nematode resistance in plants: the battle underground," *Trends in Genetics*, vol. 22, no. 7, pp. 396–403, 2006.

[11] V. P. Klink, C. C. Overall, and B. F. Matthews, "Developing a systems biology approach to study disease progression caused by *Heterodera glycines* in *Glycine max*," *Gene Regulation and Systems Biology*, vol. 2, pp. 17–33, 2007.

[12] V. P. Klink and B. F. Matthews, "Emerging approaches to broaden resistance of soybean to soybean cyst nematode as supported by gene expression studies," *Plant Physiology*, vol. 151, no. 3, pp. 1017–1022, 2009.

[13] P. Abad, J. Gouzy, J.-M. Aury, et al., "Genome sequence of the metazoan plant-parasitic nematode *Meloidogyne incognita*," *Nature Biotechnology*, vol. 26, no. 8, pp. 909–915, 2008.

[14] J. A. Wrather and S. R. Koenning, "Estimates of disease effects on soybean yields in the United States 2003–2005," *Journal of Nematology*, vol. 38, no. 2, pp. 173–180, 2006.

[15] V. C. Concibido, B. W. Diers, and P. R. Arelli, "A decade of QTL mapping for cyst nematode resistance in soybean," *Crop Science*, vol. 44, no. 4, pp. 1121–1131, 2004.

[16] B. E. Caldwell, C. A. Brim, and J. P. Ross, "Inheritance of resistance of soybeans to the soybean cyst nematode, *Heterodera glycines*," *Agronomy Journal*, vol. 52, pp. 635–636, 1960.

[17] A. L. Matson and L. F. Williams, "Evidence of a fourth gene for resistance to the soybean cyst nematode," *Crop Science*, vol. 5, article 477, 1965.

[18] A. P. Rao-Arrelli, "Inheritance of resistance to *Heterodera glycines* race 3 in soybean accessions," *Plant Disease*, vol. 78, no. 9, pp. 898–900, 1994.

[19] I. Schuster, R. V. Abdelnoor, S. R. R. Marin, et al., "Identification of a new major QTL associated with resistance to soybean cyst nematode (*Heterodera glycines*)," *Theoretical and Applied Genetics*, vol. 102, no. 1, pp. 91–96, 2001.

[20] V. C. Concibido, "DNA marker analysis of loci underlying resistance to soybean cyst nematode (*Heterodera glycines* Ichinohe)," *Crop Science*, vol. 34, no. 1, pp. 240–246, 1994.

[21] P. B. Cregan, J. Mudge, E. W. Fickus, D. Danesh, R. Denny, and N. D. Young, "Two simple sequence repeat markers to select for soybean cyst nematode resistance coditioned by the rhg1 locus," *Theoretical and Applied Genetics*, vol. 99, no. 5, pp. 811–818, 1999.

[22] R. Khan, N. Alkharouf, H. Beard, et al., "Microarray analysis of gene expression in soybean roots susceptible to the soybean cyst nematode two days post invasion," *Journal of Nematology*, vol. 36, no. 3, pp. 241–248, 2004.

[23] N. W. Alkharouf, V. P. Klink, I. B. Chouikha, et al., "Time-course microarray analyses reveal global changes in gene expression of susceptible *Glycine max* (soybean) roots during infection by *Heterodera glycines* (soybean cyst nematode)," *Planta*, vol. 224, no. 4, pp. 838–852, 2006.

[24] N. Ithal, J. Recknor, D. Nettleton, et al., "Parallel genome-wide expression profiling of host and pathogen during soybean cyst nematode infection of soybean," *Molecular Plant-Microbe Interactions*, vol. 20, no. 3, pp. 293–305, 2007.

[25] V. P. Klink, C. C. Overall, N. Alkharouf, M. H. MacDonald, and B. F. Matthews, "A comparative microarray analysis of an incompatible and compatible disease response by soybean (*Glycine max*) to soybean cyst nematode (*Heterodera glycines*) infection," *Planta*, vol. 226, pp. 1423–1447, 2007.

[26] V. P. Klink, C. C. Overall, N. W. Alkharouf, M. H. MacDonald, and B. F. Matthews, "Laser capture microdissection (LCM) and comparative microarray expression analysis of syncytial cells isolated from incompatible and compatible soybean (*Glycine max*) roots infected by the soybean cyst nematode (*Heterodera glycines*)," *Planta*, vol. 226, no. 6, pp. 1389–1409, 2007.

[27] B. Y. Endo, "Histological responses of resistant and susceptible soybean varieties, and backcross progeny to entry development of *Heterodera glycines*," *Phytopathology*, vol. 55, pp. 375–381, 1965.

[28] T. Endo, "Ultrastructure of initial responses of resistant and susceptible soybean roots to infection by *Heterodera glycines*," *Review of Plant Nematology*, vol. 14, pp. 73–94, 1991.

[29] R. D. Riggs, K. S. Kim, and I. Gipson, "Ultrastructural changes in Peking soybeans infected with *Heterodera glycines*," *Phytopathology*, vol. 63, pp. 76–84, 1973.

[30] Y. H. Kim, R. D. Riggs, and K. S. Kim, "Structural changes associated with resistance of soybean to *Heterodera glycines*," *Journal of Nematology*, vol. 19, pp. 177–187, 1987.

[31] V. P. Klink, P. Hosseini, M. H. MacDonald, N. W. Alkharouf, and B. F. Matthews, "Population-specific gene expression in the plant pathogenic nematode *Heterodera glycines* exists prior to infection and during the onset of a resistant or susceptible reaction in the roots of the *Glycine max* genotype Peking," *BMC Genomics*, vol. 10, article 111, 2009.

[32] V. P. Klink, K.-H. Kim, V. Martins, et al., "A correlation between host-mediated expression of parasite genes as tandem inverted repeats and abrogation of development of female *Heterodera glycines* cyst formation during infection of *Glycine max*," *Planta*, vol. 230, no. 1, pp. 53–71, 2009.

[33] V. P. Klink, P. Hosseini, P. Matsye, N. W. Alkharouf, and B. F. Matthews, "A gene expression analysis of syncytia laser microdissected from the roots of the *Glycine max* (soybean) genotype PI 548402 (Peking) undergoing a resistant reaction after infection by *Heterodera glycines* (soybean cyst nematode)," *Plant Molecular Biology*, vol. 71, no. 6, pp. 525–567, 2009.

[34] R. D. Riggs and D. P. Schmitt, "Optimization of the Heterodera glycines race test procedure," *Journal of Nematology*, vol. 23, pp. 149–154, 1991.

[35] T. L. Niblack, P. R. Arelli, G. R. Noel, et al., "A revised classification scheme for genetically diverse populations of *Heterodera glycines*," *Journal of Nematology*, vol. 34, no. 4, pp. 279–288, 2002.

[36] B. Y. Endo, "Penetration and development of *Heterodera glycines* in soybean roots and related and related anatomical changes," *Phytopathology*, vol. 54, pp. 79–88, 1964.

[37] M. A. Wilson, D. M. Bird, and E. van der Knaap, "A comprehensive subtractive cDNA cloning approach to identify nematode-induced transcripts in tomato," *Phytopathology*, vol. 84, no. 3, pp. 299–303, 1994.

[38] D. M. Bird and M. A. Wilson, "DNA sequence and expression analysis of root-knot nematode-elicited giant cell transcripts," *Molecular Plant-Microbe Interactions*, vol. 7, no. 3, pp. 419–424, 1994.

[39] G. Isenberg, W. Bielser, W. Meier-Ruge, and E. Remy, "Cell surgery by laser micro dissection: a preparative method," *Journal of Microscopy*, vol. 107, no. 1, pp. 19–24, 1976.

[40] W. Meier Ruge, W. Bielser, E. Remy, F. Hillenkamp, R. Nitsche, and R. Unsold, "The laser in the Lowry technique for microdissection of freeze dried tissue slices," *Histochemical Journal*, vol. 8, no. 4, pp. 387–401, 1976.

[41] M. R. Emmert-Buck, R. F. Bonner, P. D. Smith, et al., "Laser capture microdissection," *Science*, vol. 274, no. 5289, pp. 998–1001, 1996.

[42] T. Asano, T. Masumura, H. Kusano, et al., "Construction of a specialized cDNA library from plant cells isolated by laser capture microdissection: toward comprehensive analysis of the genes expressed in the rice phloem," *Plant Journal*, vol. 32, no. 3, pp. 401–408, 2002.

[43] V. P. Klink, N. Alkharouf, M. MacDonald, and B. Matthews, "Laser Capture Microdissection (LCM) and expression analyses of *Glycine max* (soybean) syncytium containing root regions formed by the plant pathogen *Heterodera glycines* (soybean cyst nematode)," *Plant Molecular Biology*, vol. 59, no. 6, pp. 965–979, 2005.

[44] V. P. Klink, P. Hosseini, P. D. Matsye, N. W. Alkharouf, and B. F. Matthews, "Syncytium gene expression in *Glycine max*$_{[PI\ 88788]}$ roots undergoing a resistant reaction to the parasitic nematode *Heterodera glycines*," *Plant Physiology and Biochemistry*, vol. 48, no. 2-3, pp. 176–193, 2010.

[45] B. F. Matthews, M. H. MacDonald, V. K. Thai, and M. L. Tucker, "Molecular characterization of argenine kinase in the soybean cyst nematode (*Heterodera glycines*)," *Journal of Nematology*, vol. 35, no. 3, pp. 252–258, 2003.

[46] N. Alkharouf, R. Khan, and B. Matthews, "Analysis of expressed sequence tags from roots of resistant soybean infected by the soybean cyst nematode," *Genome*, vol. 47, no. 2, pp. 380–388, 2004.

[47] A. M. Golden, J. M. Epps, R. D. Riggs, L. A. Duclos, J. A. Fox, and R. L. Bernard, "Terminology and identity of infraspecific forms of the soybean cyst nematode (*Heterodera glycines*)," *Plant Disease Reporter*, vol. 54, pp. 544–546, 1970.

[48] B. W. Diers, P. R. Arelli, and T. J. Kisha, "Genetic mapping of soybean cyst nematode resistance genes from PI 88788," *Soybean Genetics Newsletter*, vol. 24, pp. 194–195, 1997.

[49] N. W. Alkharouf, V. P. Klink, and B. F. Matthews, "Identification of *Heterodera glycines* (soybean cyst nematode [SCN]) cDNA sequences with high identity to those of Caenorhabditis elegans having lethal mutant or RNAi phenotypes," *Experimental Parasitology*, vol. 115, no. 3, pp. 247–258, 2007.

[50] T. L. Niblack, R. D. Heinz, G. S. Smith, and P. A. Donald, "Distribution, density, and diversity of *Heterodera glycines* in Missouri," *Journal of Nematology*, vol. 25, no. 4, supplement, pp. 880–886, 1993.

[51] S. Sardanelli and W. J. Kenworthy, "Soil moisture control and direct seeding for bioassay of *Heterodera glycines* on soybean," *Journal of Nematology*, vol. 29, no. 4, supplement, pp. 625–634, 1997.

[52] J. E. Sass, *Botanical Microtechnique*, Iowa State College Press, Ames, Iowa, USA, 1958.

[53] K. Sugimoto, R. E. Williamson, and G. O. Wasteneys, "New techniques enable comparative analysis of microtubule orientation, wall texture, and growth rate in intact roots of *Arabidopsis*," *Plant Physiology*, vol. 124, no. 4, pp. 1493–1506, 2000.

[54] M. A. Harris, J. Clark, A. Ireland, et al., "The Gene Oncology (GO) database and informatics resource," *Nucleic Acids Research*, vol. 32, pp. D258–D261, 2004.

[55] S. F. Altschul, T. L. Madden, A. A. Schäffer, et al., "Gapped BLAST and PSI-BLAST: a new generation of protein database search programs," *Nucleic Acids Research*, vol. 25, no. 17, pp. 3389–3402, 1997.

[56] N. W. Alkharouf and B. F. Matthews, "SGMD: the soybean genomics and microarray database," *Nucleic Acids Research*, vol. 32, pp. D398–D400, 2004.

[57] B. Y. Endo, "Synthesis of nucleic acids at infection sites of soybean roots parasitized by *Heterodera glycines*," *Phytopathology*, vol. 61, pp. 395–399, 1971.

[58] B. Y. Endo, *Atlas on Ultrastructure of Infective Juveniles of the Soybean Cyst Nematode Heterodera glycines*, Agricultural Handbook no. 711, 1998.

[59] T. Endo and J. A. Veech, "Morphology and histochemistry of soybean roots infected with *Heterodera glycines*," *Phytopathology*, vol. 60, no. 18, pp. 1493–1498, 1970.

[60] I. Gipson, K. S. Kim, and R. D. Riggs, "An ultrastructural study of syncytium development in soybean roots infected with *Heterodera glycines*," *Journal of Phytopathology*, vol. 61, pp. 347–353, 1971.

[61] M. G. Jones and D. H. Northcote, "Nematode-induced syncytium—a multinucleate transfer cell," *Journal of Cell Science*, vol. 10, no. 3, pp. 789–809, 1972.

[62] M. Scheideler, N. L. Schlaich, K. Fellenberg, et al., "Monitoring the switch from housekeeping to pathogen defense metabolism in *Arabidopsis thaliana* using cDNA arrays," *The Journal of Biological Chemistry*, vol. 277, no. 12, pp. 10555–10561, 2002.

[63] Y. Tao, Z. Xie, W. Chen, et al., "Quantitative nature of *Arabidopsis* responses during compatible and incompatible interactions with the bacterial pathogen Pseudomonas syringae," *Plant Cell*, vol. 15, no. 2, pp. 317–330, 2003.

[64] A. J. Afzal, A. Natarajan, N. Saini, et al., "The nematode resistance allele at the *rhg1* locus alters the proteome and primary metabolism of soybean roots," *Plant Physiology*, vol. 151, no. 3, pp. 1264–1280, 2009.

[65] E. Yamamoto and H. T. Knap, "Soybean receptor-like protein kinase genes: paralogous divergence of a gene family," *Molecular Biology and Evolution*, vol. 18, no. 8, pp. 1522–1531, 2001.

[66] C. C. Chiang and L. A. Hadwiger, "Cloning and characterization of a disease resistance response gene in pea inducible by *Fusarium solani*," *Molecular Plant-Microbe Interactions*, vol. 3, no. 2, pp. 78–85, 1990.

[67] F. Xiao, M. Lu, J. Li, et al., "Pto mutants differentially activate Prf-dependent, avrPto-independent resistance and gene-for-gene resistance," *Plant Physiology*, vol. 131, no. 3, pp. 1239–1249, 2003.

[68] P. Veronese, H. Nakagami, B. Bluhm, et al., "The membrane-anchored BOTRYTIS-INDUCED KINASE1 plays distinct roles in *Arabidopsis* resistance to necrotrophic and biotrophic pathogens," *Plant Cell*, vol. 18, no. 1, pp. 257–273, 2006.

[69] V. K. Thara, X. Tang, Y. Q. Gu, G. B. Martin, and J. M. Zhou, "*Pseudomonas syringae* pv tomato induces the expression of tomato EREBP-like genes Pti4 and Pti5 independent of ethylene, salicylate and jasmonate," *Plant Journal*, vol. 20, no. 4, pp. 475–483, 1999.

[70] J. Zhou, Y. T. Loh, R. A. Bressan, and G. B. Martin, "The tomato gene Pti1 encodes a serine/threonine kinase that is phosphorylated by Pto and is involved in the hypersensitive response," *Cell*, vol. 83, no. 6, pp. 925–935, 1995.

[71] A. F. Bent, B. N. Kunkel, D. Dahlbeck, et al., "RPS2 of *Arabidopsis thaliana*: a leucine-rich repeat class of plant disease resistance genes," *Science*, vol. 265, no. 5180, pp. 1856–1860, 1994.

[72] D. A. Jones, C. M. Thomas, K. E. Hammond-Kosack, P. J. Balint-Kurti, and J. D. G. Jonest, "Isolation of the tomato Cf-9 gene for resistance to *Cladosporium fulvum* by transposon tagging," *Science*, vol. 266, no. 5186, pp. 789–793, 1994.

[73] D. Cai, M. Kleine, S. Kifle, et al., "Positional cloning of a gene for nematode resistance in sugar beet," *Science*, vol. 275, no. 5301, pp. 832–834, 1997.

[74] S. B. Milligan, J. Bodeau, J. Yaghoobi, I. Kaloshian, P. Zabel, and V. M. Williamson, "The root knot nematode resistance gene Mi from tomato is a member of the leucine zipper, nucleotide binding, leucine-rich repeat family of plant genes," *Plant Cell*, vol. 10, no. 8, pp. 1307–1319, 1998.

[75] C. F. Hwang, A. V. Bhakta, G. M. Truesdell, W. M. Pudlo, and V. M. Williamson, "Evidence for a role of the N terminus and leucine-rich repeat region of the Mi gene product in regulation of localized cell death," *Plant Cell*, vol. 12, no. 8, pp. 1319–1329, 2000.

[76] E. A. G. van der Vossen, J. N. van der Voort, K. Kanyuka, et al., "Homologues of a single resistance-gene cluster in potato confer resistance to distinct pathogens: a virus and a nematode," *Plant Journal*, vol. 23, no. 5, pp. 567–576, 2000.

[77] K. Ernst, A. Kumar, D. Kriseleit, D.-U. Kloos, M. S. Phillips, and M. W. Ganal, "The broad-spectrum potato cyst nematode resistance gene (Hero) from tomato is the only member of a large gene family of NBS-LRR genes with an unusual amino acid repeat in the LRR region," *Plant Journal*, vol. 31, no. 2, pp. 127–136, 2002.

[78] C.-F. Hwang and V. M. Williamson, "Leucine-rich repeat-mediated intramolecular interactions in nematode recognition and cell death signaling by the tomato resistance protein Mi," *Plant Journal*, vol. 34, no. 5, pp. 585–593, 2003.

[79] G. G. Yannarelli, G. O. Noriega, A. Batlle, and M. L. Tomaro, "Heme oxygenase up-regulation in ultraviolet-B irradiated soybean plants involves reactive oxygen species," *Planta*, vol. 224, no. 5, pp. 1154–1162, 2006.

[80] Q. Pang, J. B. Hays, and I. Rajagopal, "A plant cDNA that partially complements *Escherichia coli* recA mutations predicts

a polypeptide not strongly homologous to RecA proteins," *Proceedings of the National Academy of Sciences of the United States of America*, vol. 89, no. 17, pp. 8073–8077, 1992.

[81] Q. Pang, J. B. Hays, I. Rajagopal, and T. S. Schaefer, "Selection of *Arabidopsis* cDNAs that partially correct phenotypes of *Escherichia coli* DNA-damage-sensitive mutants and analysis of two plant cDNAs that appear to express UV-specific dark repari activities," *Plant Molecular Biology*, vol. 22, no. 3, pp. 411–426, 1993.

[82] A. J. Vigers, W. K. Roberts, and C. P. Selitrennikoff, "A new family of plant antifungal proteins," *Molecular Plant-Microbe Interactions*, vol. 4, no. 4, pp. 315–323, 1991.

[83] A. Sugimoto, R. R. Hozak, T. Nakashima, T. Nishimoto, and J. H. Rothman, "dad-1, an endogenous programmed cell death suppressor in *Caenorhabditis elegans* and vertebrates," *EMBO Journal*, vol. 14, no. 18, pp. 4434–4441, 1995.

[84] D. Orzaez and A. Granell, "The plant homologue of the defender against apoptotic death gene is down-regulated during senescence of flower petals," *FEBS Letters*, vol. 404, no. 2-3, pp. 275–278, 1997.

[85] A. Danon, V. I. Rotari, A. Gordon, N. Mailhac, and P. Gallois, "Ultraviolet-C overexposure induces programmed cell death in *Arabidopsis*, which is mediated by caspase-like activities and which can be suppressed by caspase inhibitors, p35 and defender against apoptotic death," *The Journal of Biological Chemistry*, vol. 279, no. 1, pp. 779–787, 2004.

[86] C. P. Constabel, D. R. Bergey, and C. A. Ryan, "Systemin activates synthesis of wound-inducible tomato leaf polyphenol oxidase via the octadecanoid defense signaling pathway," *Proceedings of the National Academy of Sciences of the United States of America*, vol. 92, no. 2, pp. 407–411, 1995.

[87] C. P. Constabel, L. Yip, J. J. Patton, and M. E. Christopher, "Polyphenol oxidase from hybrid poplar. Cloning and expression in response to wounding and herbivory," *Plant Physiology*, vol. 124, no. 1, pp. 285–295, 2000.

[88] J. Wang and C. P. Constabel, "Polyphenol oxidase overexpression in transgenic *Populus* enhances resistance to herbivory by forest tent caterpillar (*Malacosoma disstria*)," *Planta*, vol. 220, no. 1, pp. 87–96, 2004.

[89] T. Romeis, A. A. Ludwig, R. Martin, and J. D. G. Jones, "Calcium-dependent protein kinases play an essential role in a plant defence response," *EMBO Journal*, vol. 20, no. 20, pp. 5556–5567, 2001.

[90] S. Ivashuta, J. Liu, J. Liu, et al., "RNA interference identifies a calcium-dependent protein kinase involved in *Medicago truncatula* root development," *Plant Cell*, vol. 17, no. 11, pp. 2911–2921, 2005.

[91] N. Wei and X. W. Deng, "COP9: a new genetic locus involved in light-regulated development and gene expression in *Arabidopsis*," *Plant Cell*, vol. 4, no. 12, pp. 1507–1518, 1992.

[92] Y. Liu, M. Schiff, G. Serino, X.-W. Deng, and S. P. Dinesh-Kumar, "Role of SCF ubiquitin-ligase and the COP9 signalosome in the N gene-mediated resistance response to Tobacco mosaic virus," *Plant Cell*, vol. 14, no. 7, pp. 1483–1496, 2002.

[93] D. Wang, N. Amornsiripanitch, and X. Dong, "A genomic approach to identify regulatory nodes in the transcriptional network of systemic acquired resistance in plants," *PLoS Pathogens*, vol. 2, article e123, 2006.

[94] Z. Zheng, S. A. Qamar, Z. Chen, and T. Mengiste, "*Arabidopsis* WRKY33 transcription factor is required for resistance to necrotrophic fungal pathogens," *Plant Journal*, vol. 48, no. 4, pp. 592–605, 2006.

[95] X. Liu, X. Bai, X. Wang, and C. Chu, "OsWRKY71, a rice transcription factor, is involved in rice defense response," *Journal of Plant Physiology*, vol. 164, no. 8, pp. 969–979, 2007.

[96] H. S. Ryu, M. Han, S. K. Lee, et al., "A comprehensive expression analysis of the WRKY gene superfamily in rice plants during defense response," *Plant Cell Reports*, vol. 25, no. 8, pp. 836–847, 2006.

[97] S.-K. Oh, S. Y. Yi, S. H. Yu, J. S. Moon, J. M. Park, and D. Choi, "CaWRKY2, a chili pepper transcription factor, is rapidly induced by incompatible plant pathogens," *Molecules and Cells*, vol. 22, no. 1, pp. 58–64, 2006.

[98] B. Ulker, M. Shahid Mukhtar, and I. E. Somssich, "The WRKY70 transcription factor of *Arabidopsis* influences both the plant senescence and defense signaling pathways," *Planta*, vol. 226, no. 1, pp. 125–137, 2007.

[99] M. Shimono, S. Sugano, A. Nakayama, et al., "Rice WRKY45 plays a crucial role in benzothiadiazole-inducible blast resistance," *Plant Cell*, vol. 19, no. 6, pp. 2064–2076, 2007.

[100] H. Cao, S. A. Bowling, A. S. Gordon, and X. Dong, "Characterization of an *Arabidopsis* mutant that is nonresponsive to inducers of systemic acquired resistance," *Plant Cell*, vol. 6, no. 11, pp. 1583–1592, 1994.

[101] K. C. Vaughn and S. O. Duke, "Function of polyphenol oxidase in higher plants," *Plant Physiology*, vol. 60, pp. 106–112, 1984.

[102] D. F. Hildebrand, J. G. Rodriguez, G. C. Brown, K. Y. Lui, and C. S. Volden, "Peroxidative responses of leaves in two soybean genotypes injured by two spotted spider mites (Acari: Tetranychidae)," *Journal of Economic Entomology*, vol. 79, pp. 1459–1465, 1986.

[103] A. M. Mayer, "Polyphenol oxidases in plants-recent progress," *Phytochemistry*, vol. 26, no. 1, pp. 11–20, 1987.

[104] G. W. Felton, K. Donato, R. J. Del Vecchio, and S. S. Duffey, "Activation of plant foliar oxidases by insect feeding reduces nutritive quality of foliage for noctuid herbivores," *Journal of Chemical Ecology*, vol. 15, no. 12, pp. 2667–2694, 1989.

[105] S. S. Duffey and G. W. Felton, "Enzymatic antinutritive defenses of the tomato plant against insects," in *Naturally Occurring Pest Bioregulators*, P. A. Hedin, Ed., pp. 167–197, ACS, Washington, DC, USA, 1991.

[106] S. S. Duffey and M. J. Stout, "A nutritive and toxic compounds of plant defense against insects," *Archives of Insect Biochemistry and Physiology*, vol. 32, pp. 3–37, 1996.

[107] L. Li and J.C. Steffens, "Overexpression of polyphenol oxidase in transgenic tomato plants results in enhanced bacterial disease resista," *Planta* , vol. 215, no. 2, pp. 239–247, 2002.

[108] Q.-H. Shen, Y. Saijo, S. Mauch, et al., "Nuclear activity of MLA immune receptors links isolate-specific and basal disease-resistance responses," *Science*, vol. 315, no. 5815, pp. 1098–1103, 2007.

[109] J. Ryals, K. Weymann, K. Lawton, et al., "The *Arabidopsis* NIM1 protein shows homology to the mammalian transcription factor inhibitor IκB," *Plant Cell*, vol. 9, no. 3, pp. 425–439, 1997.

[110] J. Shah, F. Tsui, and D. F. Klessig, "Characterization of a salicylic acid-insensitive mutant (*sai1*) of *Arabidopsis thaliana*, identified in a selective screen utilizing the SA-inducible expression of the tms2 gene," *Molecular Plant-Microbe Interactions*, vol. 10, no. 1, pp. 69–78, 1997.

[111] T. P. Delaney, L. Friedrich, and J. A. Ryals, "Arabidopsis signal transduction mutant defective in chemically and biologically induced disease resistance," *Proceedings of the National Academy of Sciences of the United States of America*, vol. 92, no. 14, pp. 6602–6606, 1995.

[112] J. Glazebrook, E. E. Rogers, and F. M. Ausubel, "Isolation of *Arabidopsis* mutants with enhanced disease susceptibility by direct screening," *Genetics*, vol. 143, no. 2, pp. 973–982, 1996.

[113] Z. Mou, W. Fan, and X. Dong, "Inducers of plant systemic acquired resistance regulate NPR1 function through redox changes," *Cell*, vol. 113, no. 7, pp. 935–944, 2003.

[114] Y. Tada, S. H. Spoel, K. Pajerowska-Mukhtar, et al., "Plant immunity requires conformational charges of NPR1 via S-nitrosylation and thioredoxins," *Science*, vol. 321, no. 5891, pp. 952–956, 2008.

[115] M. J. E. Wubben, J. Jin, and T. J. Baum, "Cyst nematode parasitism of *Arabidopsis thaliana* is inhibited by salicylic acid (SA) and elicits uncoupled SA-independent pathogenesis-related gene expression in roots," *Molecular Plant-Microbe Interactions*, vol. 21, no. 4, pp. 424–432, 2008.

[116] N. Bouché, A. Yellin, W. A. Snedden, and H. Fromm, "Plant-specific calmodulin-binding proteins," *Annual Review of Plant Biology*, vol. 56, pp. 435–466, 2005.

[117] P. De Koninck and H. Schulman, "Sensitivity of CaM kinase II to the frequency of Ca^{2+} oscillations," *Science*, vol. 279, no. 5348, pp. 227–230, 1998.

[118] J. Lévy, C. Bres, R. Geurts, et al., "A putative Ca^{2+} and calmodulin dependent protein kinase required for bacterial and fungal symbioses," *Science*, vol. 303, no. 5662, pp. 1361–1364, 2004.

[119] D. Mitra and M. M. Johri, "Enhanced expression of a calcium-dependent protein kinase from the moss *Funaria hygrometrica* under nutritional starvation," *Journal of Biosciences*, vol. 25, no. 4, pp. 331–338, 2000.

[120] V. P. Klink, M. H. MacDonald, V. E. Martins, et al., "MiniMax, a new diminutive *Glycine max* genotype with a rapid life cycle, embryogenic potential and transformation capabilities," *Plant Cell, Tissue and Organ Culture*, vol. 92, no. 2, pp. 183–195, 2008.